THE UNIVERSITY of EDINBURGH

Edinburgh Research Explorer

Genome-wide association meta-analysis highlights light-induced signaling as a driver for refractive error

Citation for published version:
CREAM Consortium, Tedja, MS, Wojciechowski, R, Hysi, PG, Eriksson, N, Furlotte, NA, Verhoeven, VJM, Iglesias, AI, Meester-Smoor, MA, Tompson, SW, Fan, Q, Khawaja, AP, Cheng, C-Y, Höhn, R, Yamashiro, K, Wenocur, A, Grazal, C, Haller, T, Metspalu, A, Wedenoja, J, Jonas, JB, Wang, YX, Xie, J, Mitchell, P, Foster, PJ, Klein, BEK, Klein, R, Paterson, AD, Hosseini, SM, Shah, RL, Williams, C, Teo, YY, Tham, YC, Gupta, P, Zhao, W, Shi, Y, Saw, W-Y, Tai, E-S, Sim, XL, Huffman, JE, Polašek, O, Hayward, C, Bencic, G, Rudan, I, Wilson, JF, Joshi, PK, Tsujikawa, A, Matsuda, F, Whisenhunt, KN, Zeller, T & Vitart, V 2018, 'Genome-wide association meta-analysis highlights light-induced signaling as a driver for refractive error', *Nature Genetics*, vol. 50, pp. 834-848. https://doi.org/10.1038/s41588-018-0127-7

Digital Object Identifier (DOI):
10.1038/s41588-018-0127-7

Link:
Link to publication record in Edinburgh Research Explorer

Document Version:
Peer reviewed version

Published In:
Nature Genetics

Publisher Rights Statement:
This is the author’s peer-reviewed manuscript as accepted for publication.

General rights
Copyright for the publications made accessible via the Edinburgh Research Explorer is retained by the author(s) and / or other copyright owners and it is a condition of accessing these publications that users recognise and abide by the legal requirements associated with these rights.

Take down policy
The University of Edinburgh has made every reasonable effort to ensure that Edinburgh Research Explorer content complies with UK legislation. If you believe that the public display of this file breaches copyright please contact openaccess@ed.ac.uk providing details, and we will remove access to the work immediately and investigate your claim.

Download date: 27. Aug. 2022

1 # Large genome-wide meta-analysis highlights
2 # light-induced signaling as a driver for
3 # refractive error

4 Milly S. Tedja[1,2,76], Robert Wojciechowski[3,4,76], Pirro G. Hysi[5,76], Nicholas Eriksson[6,76], Nicholas A.
5 Furlotte[6,76], Virginie J.M. Verhoeven[1,2,7,76], Stuart W.J. Tompson[8], Adriana I. Iglesias Gonzalez[2], Qiao
6 Fan[9], Anthony P. Khawaja[10], Ching-Yu Cheng[9,11], René Höhn[12,13], Elisabeth M. van Leeuwen[1,2], Kenji
7 Yamashiro[14], Adam Wenocur[15], Clare Grazal[15], Toomas Haller[16], Andres Metspalu[16], Juho Wedenoja[17,18],
8 Jost B. Jonas[19,20], Ya Xing Wang[20], Jing Xie[21], Paul Mitchell[22], Paul J. Foster[23], Barbara E.K. Klein[8],
9 Ronald Klein[8], Andrew D. Paterson[24], Mohsen S. Hosseini[24], Rupal L. Shah[25], Cathy Williams[26], Yik
10 Ying Teo[27,28], Yih Chung Tham[11], Preeti Gupta[29], Wanting Zhao[30], Yuan Shi[30], Woei-Yuh Saw[31], E
11 Shyong Tai[28], Xue Ling Sim[28], Jennifer E. Huffman[32], Ozren Polašek[33], Caroline Hayward[32], Goran
12 Bencic[34], Igor Rudan[35], James F. Wilson[35], CREAM[#], 23andMe Research Team, Peter K. Joshi[35], Akitaka
13 Tsujikawa[14], Fumihiko Matsuda[36], Kristina N. Whisenhunt[8], Tanja Zeller[37], Peter J. van der Spek[38],
14 Roxanna Haak[38], Arthur A. B. Bergen[39,40], Hanne Meijers-Heijboer[40,41], Magda A. Meester-Smoor[1,2],
15 Sudha K. Iyengar[42-44], Jonathan H. Lass[42,43], Albert Hofman[2,45,46], Fernando Rivadeneira[2,46,47], André G.
16 Uitterlinden[2,46,47], Johannes R. Vingerling[1], Terho Lehtimäki[48,49], Olli T. Raitakari[50,51], Ginevra Biino[52],
17 Maria Pina Concas[53], Tae Hwi Schwantes-An[4,54], Robert P. Igo, Jr.[42], Gabriel Cuellar[55], Nicholas G.
18 Martin[56], Jamie E. Craig[57], Puya Gharahkhani[55], Katie M. Williams[5], Abhishek Nag[58], Jugnoo S. Rahi[59],
19 Phillippa Cumberland[59], Cécile Delcourt[60], Céline Bellenguez[61-63], Janina S. Ried[64], Thomas
20 Meitinger[65,66], Christian Gieger[64], Tien Yin Wong[67,68], Alex W. Hewitt[21,69], David A. Mackey[70], Claire L.
21 Simpson[4,71], Norbert Pfeiffer[13], Olavi Pärssinen[72,73], Paul N. Baird[21], Veronique Vitart[32], Najaf Amin[2],
22 Cornelia M. van Duijn[2], Joan E. Bailey-Wilson[4], Terri L. Young[8], Seang Mei Saw [28,74], Dwight
23 Stambolian[15], Stuart MacGregor[55], Jeremy A. Guggenheim[25,77], Joyce Tung[6,77], Christopher J.
24 Hammond[5,77], Caroline C.W. Klaver[1,2,75,77]

25

Affiliations

1. Department of Ophthalmology, Erasmus Medical Center, Rotterdam, The Netherlands.
2. Department of Epidemiology, Erasmus Medical Center, Rotterdam, The Netherlands.
3. Department of Epidemiology and Medicine, Johns Hopkins Bloomberg School of Public Health, Baltimore, Maryland, USA.
4. Computational and Statistical Genomics Branch, National Human Genome Research Institute, National Institutes of Health, Bethesda, Maryland, USA.
5. Department of Ophthalmology, King's College London, London, UK.
6. 23andMe, Inc., Mountain View, USA.
7. Department of Clinical Genetics, Erasmus Medical Center, Rotterdam, The Netherlands.
8. Department of Ophthalmology and Visual Sciences, University of Wisconsin School of Medicine and Public Health, Madison, Wisconsin, USA.
9. Ophthalmology & Visual Sciences Academic Clinical Program and Centre for Quantitative Medicine, DUKE-National University of Singapore, Singapore.
10. Department of Public Health and Primary Care, University of Cambridge, Cambridge, UK.
11. Ocular Epidemiology Research Group, Singapore Eye Research Institute, Singapore National Eye Centre, Singapore, Singapore.
12. Department of Ophthalmology, University Hospital Bern, Inselspital, University of Bern, Bern, Switzerland.
13. Department of Ophthalmology, University Medical Center Mainz, Mainz, Germany.
14. Department of Ophthalmology and Visual Sciences, Kyoto University Graduate School of Medicine, Kyoto, Japan.
15. Department of Ophthalmology, University of Pennsylvania, Philadelphia, Pennsylvania, USA.
16. Estonian Genome Center, University of Tartu, Tartu, Estonia.
17. Department of Ophthalmology, Helsinki University Hospital, University of Helsinki, Helsinki, Finland.
18. Department of Public Health, University of Helsinki, Helsinki, Finland.
19. Department of Ophthalmology, Medical Faculty Mannheim of the Ruprecht-Karls-University of Heidelberg, Mannheim, Germany.
20. Beijing Institute of Ophthalmology, Beijing Key Laboratory of Ophthalmology and Visual Sciences, Beijing Tongren Eye Center, Beijing Tongren Hospital, Capital Medical University, Beijing, China.
21. Centre for Eye Research Australia, University of Melbourne, Melbourne, Australia.
22. Department of Ophthalmology, Centre for Vision Research, Westmead Institute for Medical Research, University of Sydney, Sydney, Australia.
23. NIHR Biomedical Research Centre, Moorfields Eye Hospital NHS Foundation Trust and UCL Institute of Ophthalmology, London, UK.
24. Program in Genetics and Genome Biology, Hospital for Sick Children and University of Toronto, Toronto, Ontario, Canada.
25. School of Optometry & Vision Sciences, Cardiff University, Cardiff, UK.
26. School of Social and Community Medicine, University of Bristol, Bristol, UK.
27. Department of Statistics and Applied Probability, National University of Singapore, Singapore, Singapore.
28. Saw Swee Hock School of Public Health, National University Health Systems, National University of Singapore, Singapore, Singapore.
29. Department of Health Service Research, Singapore Eye Research Institute, Singapore National Eye Centre, Singapore, Singapore.
30. Statistics Support Platform, Singapore Eye Research Institute, Singapore National Eye Centre, Singapore, Singapore.
31. Life Sciences Institute, National University of Singapore, Singapore, Singapore.

77 32. Institute of Genetics and Molecular Medicine, Medical Research Council Human Genetics Unit,
78 University of Edinburgh, Edinburgh, UK.
79 33. Faculty of Medicine, University of Split, Split, Croatia.
80 34. Department of Ophthalmology, Sisters of Mercy University Hospital, Zagreb, Croatia.
81 35. Centre for Global Health Research, Usher Institute for Population Health Sciences and
82 Informatics, University of Edinburgh, Edinburgh, UK.
83 36. Center for Genomic Medicine, Kyoto University Graduate School of Medicine, Kyoto, Japan.
84 37. Clinic for General and Interventional Cardiology, University Heart Center Hamburg, Hamburg,
85 Germany.
86 38. Department of Bioinformatics, Erasmus Medical Center, Rotterdam, The Netherlands.
87 39. Department of Ophthalmology, Academic Medical Center, Amsterdam, The Netherlands.
88 40. Department of Clinical Genetics, Academic Medical Center, Amsterdam, The Netherlands.
89 41. Department of Clinical Genetics, VU University Medical Center, Amsterdam, The Netherlands.
90 42. Department of Epidemiology and Biostatistics, Case Western Reserve University, Cleveland,
91 Ohio, USA.
92 43. Department of Ophthalmology and Visual Sciences, Case Western Reserve University and
93 University Hospitals Eye Institute, Cleveland, Ohio, USA.
94 44. Department of Genetics, Case Western Reserve University, Cleveland, Ohio, USA.
95 45. Department of Epidemiology, Harvard T.H. Chan School of Public Health, Boston,
96 Massachusetts, USA.
97 46. Netherlands Consortium for Healthy Ageing, Netherlands Genomics Initiative, the Hague, the
98 Netherlands.
99 47. Department of Internal Medicine, Erasmus Medical Center, Rotterdam, The Netherlands.
100 48. Department of Clinical Chemistry, University of Tampere School of Medicine, Tampere, Finland.
101 49. Department of Clinical Chemistry, Fimlab Laboratories, University of Tampere, Tampere,
102 Finland.
103 50. Research Centre of Applied and Preventive Cardiovascular Medicine, University of Turku,
104 Turku, Finland.
105 51. Department of Clinical Physiology and Nuclear Medicine, Turku University Hospital, Turku,
106 Finland.
107 52. Institute of Molecular Genetics, National Research Council of Italy, Sassari, Italy.
108 53. Institute of Genetic and Biomedical Research, National Research Council of Italy, Sassari, Italy.
109 54. Department of Medical and Molecular Genetics, Indiana University - Purdue University
110 Indianapolis, Indianapolis, Indiana, USA.
111 55. Department of Statistical Genetics, Queensland Institute of Medical Research, Brisbane,
112 Australia.
113 56. Department of Genetic Epidemiology, Queensland Institute of Medical Research, Brisbane,
114 Australia.
115 57. Department of Ophthalmology, Flinders University, Adelaide, Australia.
116 58. Department of Twin Research and Genetic Epidemiology, King's College London, London, UK.
117 59. Great Ormond Street Institute of Child Health, University College London, London, UK.
118 60. Team LEHA, UMR 1219, Université de Bordeaux, Inserm, Bordeaux Population Health
119 Research Center, Bordeaux, France.
120 61. Institut Pasteur de Lille, Lille, France.
121 62. Université de Lille, U1167, Lille, France.
122 63. Inserm, U1167, Lille, France.
123 64. Institute of Genetic Epidemiology, Helmholtz Zentrum München—German Research Center for
124 Environmental Health, Neuherberg, Germany.
125 65. Institute of Human Genetics, Helmholtz Zentrum München, Neuherberg, Germany.
126 66. Institute of Human Genetics, Klinikum rechts der Isar, Technische Universität München, Munich,
127 Germany.

128 67. Academic Medicine Research Institute, Singapore.
129 68. Retino Center, Singapore National Eye Centre, Singapore, Singapore.
130 69. Department of Ophthalmology, Menzies Institute of Medical Research, University of Tasmania,
131 Hobart, Australia.
132 70. Centre for Ophthalmology and Visual Science, Lions Eye Institute, University of Western
133 Australia, Perth, Australia.
134 71. Department of Genetics, Genomics and Informatics, University of Tennessee Health Sciences
135 Center, Memphis, Tenessee.
136 72. Department of Ophthalmology, Central Hospital of Central Finland, Jyväskylä, Finland.
137 73. Gerontology Research Center and Department of Health Sciences, University of Jyväskylä,
138 Jyväskylä, Finland.
139 74. Myopia Research Group, Singapore Eye Research Institute, Singapore National Eye Centre,
140 Singapore, Singapore.
141 75. Department of Ophthalmology, Radboud University Medical Center, Nijmegen, The Netherlands.
142 76. These authors contributed equally to this work.
143 77. These authors jointly directed this work.
144
145 [#] A full list of consortium members appears at the end of the paper.

146 **Corresponding author**

147 Prof. dr. Caroline C.W. Klaver, Erasmus Medical Center, room Na-2808, PO Box 2040, 3000 CA,

148 Rotterdam, the Netherlands, e-mail: c.c.w.klaver@erasmusmc.nl, phone number +31651934491, fax

149 number +31107044657

150

151

152

153

154

155

156

157
158

159

160

161

Abstract

Refractive errors, including myopia, are the most frequent eye disorders worldwide and an increasingly common cause of blindness. Through a genome-wide association meta-analysis in 160,420 participants of mixed ancestry from CREAM and 23andMe and replication in 95,505 participants from the UK Biobank, we increased the number of significant independent signals from 37 to 161 and found a high genetic correlation between Europeans and Asians (>0.78). Enrichment analysis identified retinal cell physiology and light processing as the most prominent mechanisms. Expression experiments and comprehensive *in silico* analyses of the novel genes showed functional contribution of all cell types in the neurosensory retina (*GNB3, DRD1, AKAP6, ZEB2, TFAP2B, CA8, EDN2*), the retinal pigment epithelium (*EFEMP1, ANO2*), vascular endothelium (*CD34, FLT1*), and extracellular matrix (*VIPR2, ANTXR2, TCF7L2, COL10A1*) to refractive error development. The newly identified genes also elicited novel mechanisms such as rod as well as cone bipolar synaptic neurotransmission (rod: *CLU*; cone: *GNB3*), anterior segment morphology (*TCF7L2, VIPR2, MAF*), and angiogenesis (*FLT1*). Twenty eight SNPs resided in or near DNA structures transcribing small RNAs (non-coding, tRNAs, snoRNas, rRNAs, miRNA), suggesting a role for post-transcriptional regulation. Our results support the notion that refractive errors are caused by a light-dependent retina-to-sclera signaling cascade, and delineate potential molecular drivers defining the pathobiology of refractive errors and myopia.

181 # Introduction

182 Refractive errors are common optical aberrations determined by mismatches in the focusing power of the
183 cornea, lens and axial length of the eye. Their distribution is rapidly shifting towards myopia, or
184 nearsightedness, all over the world. The myopia boom is particularly prominent in urban East Asia where
185 up to 95% of twenty-year-olds in cities such as Seoul and Singapore have this refractive error[1-4]. Myopia
186 prevalence is also rising throughout Western Europe and the USA, affecting ~50% of young adults in
187 these regions[5,6]. While refractive errors can be optically corrected, even at moderate values they carry a
188 significant risk of ocular complications with a high economic burden[7-9]. One in three individuals with
189 high myopia (-6 diopters or worse) will develop irreversible visual impairment or blindness, mostly due
190 to myopic macular degeneration, retinal detachment, or glaucoma[10,11]. At the other extreme, high
191 hyperopia predisposes to strabismus, amblyopia and angle-closure glaucoma[10,12].

192 Refractive errors result from a complex interplay of lifestyle and genetic factors. Most established
193 lifestyle factors for myopia are high education, lack of outdoor exposure, and excessive near work[3].
194 Recent research has identified many genetic variants for refractive errors, myopia, and axial length[13-25].
195 Two large studies, the international Consortium for Refractive Error and Myopia (CREAM)[26] and the
196 personal genomics company 23andMe, Inc.[17,27] have provided the most comprehensive results. Despite
197 differences in design and methodology, 37 associated genetic loci were identified in common, and most
198 strikingly, there was a near-linear relationship in genetic effect sizes of the associated variants[28].

199 Given that only 3.6% of the variance of the refractive error trait was explained by the identified
200 genetic variants[26], we presumed a high missing heritability. We therefore combined CREAM and
201 23andMe, and expanded the study sample to 160,420 individuals from a mixed ancestry population with
202 quantitative information on refraction for a genome-wide association (GWA) meta-analysis. Significant
203 variants were tested for replication in an independent cohort consisting of 95,505 individuals from the UK
204 Biobank. We conducted systematic comparisons to assess differences in genetic inheritance and

205 distribution of risk variants between Europeans and Asians. Polygenic risk analyses were performed to

206 evaluate the contribution of the identified variants to the risk of myopia and hyperopia. Finally, we

207 integrated expression data and bioinformatics on the identified genes to gain insight into the possible

208 mechanisms underlying the genetic associations.

209

210

211

RESULTS

Susceptibility loci for refractive error

We performed a GWAS meta-analysis on adult refractive error using summary statistics from 37 studies from the Consortium for Refractive Error and Myopia (CREAM) and two cohorts from the personal genomics company 23andMe (Supplementary Figure 1). Analyses were based on ~11 million genetic variants (SNPs, insertions and deletions) genotyped or imputed to 1000 Genomes Project Phase I reference panel (version 3, March 2012 release[29]) that passed extensive quality control (Supplementary Figures 2-5, Supplementary Table 1a) and were represented by at least half of the entire study population and by > 13 cohorts from CREAM and both cohorts from 23andMe.

Meta-analyses were conducted in three stages. *Stage 1* focused on CREAM and included a fixed effects inverse variance-weighted meta-analysis on 44,192 individuals of European descent (CREAM-EUR) and 11,935 participants of East or South Asian ancestry (CREAM-ASN) using untransformed spherical equivalent (SphE) as the dependent variable representing refractive error (Supplementary Table 1b). 1,063 variants clustering in 24 loci (Supplementary Excel File 1) were genome-wide significant (P 5 x 10^{-8}). *Stage 2* consisted of a fixed effects inversed variance-weighted meta-analysis of the two European 23andMe cohorts ($N_{23andMe_V2}$= 12,128; $N_{23andMe_V3}$ = 92,165) using age of diagnosis of myopia (AODM) as outcome[27]. A total of 5,205 genome-wide significant variants clustered in 112 loci (Supplementary Excel File 1). All 25 loci identified at Stage 1 replicated in Stage 2 (*pBonferroni* 2.00 x 10^{-3}). Vice versa, 29 (26%) of the loci identified at Stage 2 replicated in Stage 1 (*pBonferroni* 4.46 x 10^{-4}), an expected proportion given the lower statistical power in CREAM. *Stage 3* was the joint meta-analysis of Stage 1 and Stage 2. As CREAM and 23andMe applied different phenotype measures, we used signed Z-scores as the mean per-allele effect size and assigned equal weights to CREAM and 23andMe. We identified 7,967 genome-wide significant genetic variants clustering in 140 loci (Figure 1a; Supplementary Figure 5-6,

235 Supplementary Excel File 1 – 3, Supplementary PDF File 1 and 2) of which 104 were novel. All 37 loci
236 that were found previously by CREAM and 23andMe using genotype data imputed to the HapMap II
237 reference panel were replicated (*pBonferroni* 1.85 x 10^{-3}), and 36 of the 37 were genome-wide significant
238 (Supplementary Table 2)[26,27]. We applied genomic control at each stage and checked for population
239 stratification using LD score regression[30] (Supplementary Table 3). At Stage 1 and 2, population
240 stratification was unlikely as inflation factors (λGC) were < 1.1 (Supplementary Figure 7), and LD score
241 regression intercepts ($LDSC_{intercept}$) ranged from 0.892 to 1.023 (Supplementary Figure 8). At Stage 3, we
242 observed an inflation of the median test statistic (λGC=1.129; Supplementary Figure 6), probably due to
243 true polygenicity rather than bias (i.e. population stratification or cryptic relatedness)[31]. The mixed
244 ancestry did not allow for calculation of $LDSC_{intercept}$.

245 To detect the presence of multiple independent signals at the discovered loci, a stepwise
246 conditional analysis was performed with GCTA-COJO[32] on meta-analysis summary statistics from all
247 European cohorts (*N*=148,485*)* using the Rotterdam Study I-III (RS I-III) as a reference panel for LD
248 structure ($N_{RSI-III}$ = 10,775). This analysis yielded 27 additional independent variants, resulting in a total of
249 167 loci (Supplementary Excel File 1). The lead variants at the newly-discovered loci were mainly of
250 lower minor allele frequencies (MAFs) than those reported in previous refractive error GWAS studies
251 with lower samples, reflecting the increased statistical power of the current analysis (Figure 1b).

252 We advanced these loci for replication analysis in a GWAS of refractive error carried out by the
253 UK Eye & Vision (UKEV) Consortium in 95,505 participants of European ancestry from the UK
254 BioBank. [33]16 variants were not present in UKEV, and were represented by a surrogate variant in high
255 LD (r^2 >0.8 LD; Supplementary Excel File 1). Six out of the 167 variants were not considered for
256 replication analysis: one variant (rs188159083) was not present on the array nor a surrogate was available
257 in UKEV and five variants showed evidence of departure from HWE (HWE exact test $P < 3.0 \times 10^{-4}$,
258 where 3.0×10^{-4}=0.05/167). One of these five variants (rs3138141, *RDH5*) was identified previously and
259 therefore still considered as a refractive error risk variant[26,27]. The remaining 161 genetic variants were
260 tested for replication. 86% (138/161) of the candidate variants replicated significantly: 104 (65%)

261 replicated surpassing genome wide significance; 34 replicated surpassing Bonferroni correction (P < 3.0 x
262 10^{-4}; 21.1%); and, 12 showed nominal evidence for replication (0.05 < P < 3.0 x 10^{-4}; 7.5%). Of the total,
263 only 11 (7%) did not replicate (Table 1 and Supplementary Excel File 1).
264 As CREAM and 23andMe employed different phenotypic outcomes, we evaluated consistency of
265 genotypic effects by comparing marker-wise additive genetic effect sizes (in units diopters per copy of the
266 risk allele) for SphE from CREAM-EUR against those (in units log(HR) per copy of the risk allele) for
267 AODM from 23andMe. All variants strongly associated with either outcome ($P < 0.001$), were
268 concordant in direction-of-effect, and had highly correlated effect sizes (Figure 2 a,b; Supplementary
269 Figure 9). For these variants, a 10% decrease in the log(HR) for AODM, indicating an earlier age-at-
270 myopia onset, was associated with a decrease of 0.15 diopters in SphE. A quantitative analysis for all
271 common SNPs (MAF > 0.01; HapMap3) using LD score regression yielded a genetic correlation of 0.93
272 (95% CI 0.86 to 0.99; $P = 2.1 \times 10^{-159}$), confirming that effect sizes for both phenotypic outcomes were
273 closely related.
274

275 Gene annotation of susceptibility loci

276 We annotated all genetic variants with wANNOVAR using the University of California Santa Cruz
277 (UCSC) Known Gene database[34,35]. The identified 139 genetic loci were annotated to 208 genetic
278 structures (i.e. genes and known transcribed RNA genes, Table 1, Supplementary Excel file 1, Online
279 Methods). The physical positions of the lead genetic variants relative to protein-coding genes are shown
280 in Figure 1c. 86% of the identified variants were either intragenic or less than 50 kb from the 5'or 3' end
281 of the transcription start site. We found seven exonic variants (Supplementary Table 4) of which two had
282 MAF ≤ 0.05: rs5442 (*GNB3*) and rs17400325 (*PDE11A)*. The index SNP in the *GNB3* locus with MAF
283 0.05 in Europeans is a highly conserved missense variant (G272S) predicted to be damaging by
284 PolyPhen-2[36] and SIFT[37]. *PDE11A* is presumed to play a role in tumorigenesis, brain function, and
285 inflammation[38]. The index SNP in the *PDE11A* locus with MAF 0.03 in Europeans is also a highly

286 conserved missense variant (Y727C); this variant was predicted to be damaging by PolyPhen[36], SIFT[39]
287 and align GVGD[40,41].The other exonic variants, rs1064583 (*COL10A1*), rs807037 (*KAZALD1*), rs1550094
288 (*PRSS56*), rs35337422 (*RD3L*) and rs6420484 (*TSPAN10*), were not predicted to be damaging.
289 The most significant variant (Stage 3; rs12193446, $P = 4.21 \times 10^{-84}$) resides on chromosome 6
290 within a non-coding RNA, *BC035400*, in an intron of the *LAMA2* gene. This locus had been identified
291 previously, but our current fine mapping redefined the most associated variant. The function and potential
292 downstream target sites for BC035400 are currently unknown. The previously most strongly associated
293 variant, rs524952 on chromosome 15 near *GJD2*, was the second most significant variant ($P = 2.28 \times 10^{-}$
294 ^{65}).

295 Post-GWAS analyses identify 22 additional novel candidate loci

296 We performed two gene-based tests, fastBAT[42] and EUGENE[43], and applied a functional enrichment
297 approach using fgwas[44] (Online Methods). Fgwas incorporates functional annotation (eg. DNase I
298 hypersensitive sites in various tissues and 3'UTR regions) to reweight data from GWAS, and uses a
299 Bayesian model to calculate a posterior probability of association. With fastBAT, we identified 13 genes
300 at P value < 2.0×10^{-6}, one of which (*CHD7*) had been identified previously[26,27]. Using EUGENE, we
301 found 7 genes at P value < 2.0×10^{-6} after incorporation of blood eQTLs. With fgwas, we identified 6
302 loci, which could be annotated to 9 genes, at posterior probability >0.9. Two genes (*HMGN4* and *TLX1*)
303 showed significant associations in two or more approaches. Taken together, these post-GWAS approaches
304 resulted in a total of 22 additional candidate loci for refractive error, annotated to 25 genes
305 (Supplementary Table 5). This increases the overall number of significant genetic associations to 161
306 candidate loci.

307

308

309 ## Polygenic risk scores

310 We calculated polygenic risk scores (PGRS)[45] per individual at various *P* value thresholds (Online
311 Methods) for Rotterdam Study I-III (RS I-III; *N*=10,792) after recalculating *P* values and Z-scores of
312 variants from Stage 3 excluding RS I-III. We found the highest fraction of phenotypic variance (7.8%)
313 explained with 7,307 variants at *P* value threshold 0.005 (Supplementary Table 6). A PGRS based on
314 these variants distinguished well between individuals with hyperopia and myopia at the lower and higher
315 deciles (Figure 3); those in the highest decile had a 40-fold increased risk of myopia. When the PGRS
316 was stratified for the median age (< 63 or > 63+ yrs), we found a significant difference in the variance
317 explained (<63 yrs 8.9%; 63+ yrs 7.4%; *P* value 0.0038). The variance explained by PGRS was not
318 significantly different between males and females (8.3% vs 7.5%; *P* value 0.13). The predictive value
319 (area under the receiver operating characteristic curve, AUC) of the PGRS for myopia versus hyperopia
320 adjusted for age and gender was 0.77 (95% CI = 0.75–0.79), a 10% increase compared to previous
321 estimations[46].

322 ## Trans-ethnic comparison of genotypic effects

323 To explore potential ancestry differences in the identified refractive error loci, we calculated the
324 heritability explained by common genetic variants (SNP-h^2) for Europeans and Asians using LD score
325 regression[47]. SNP-h^2 was 0.214 (95% CI 0.185 to 0.243) and 0.172 (95% CI 0.154 to 0.190) in the
326 European samples (CREAM-EUR and 23andMe), while it was only 0.053 (95% CI -0.025 to 0.131) in
327 the Asian sample (CREAM-EAS). Next, we estimated the genetic correlation between Europeans and
328 Asians by comparing variant effect size for common variants using the novel statistical program
329 Popcorn[48]. Popcorn takes summary GWAS statistics from two populations and LD information from
330 ancestry-matched reference panels, and computes genetic correlations by implementing a weighted
331 likelihood function that accounts for the inflation of Z scores due to LD (Online Methods). Two genetic
332 correlation metrics were calculated (Table 2); first, a genetic effect correlation (ρge) that quantifies the

333 correlation in SNP effect sizes between Europeans and Asians without taking into account ancestry-
334 related differences in allele frequency; and second, a genetic impact correlation (ρgi) that estimates the
335 correlation in variance-normalized SNP effect sizes between the two ancestry groups. Estimates of the
336 genetic effect correlation ρge were high between Europeans and Asians, but significantly different from 1
337 (0.79 and 0.80 respectively at $P < 1.9 \times 10^{-6}$; Table 2), indicating a clear genetic overlap but a difference in
338 per allele effect size. Estimates of the genetic impact correlation ρgi were similarly high (> 0.8), but not
339 significantly different from 1 for the correlation between CREAM-EUR and CREAM-ASN ($P = 0.065$),
340 indicating that the genetic impact of these alleles may still be similar.
341

342 ## In silico pathway analysis

343 We used an array of bioinformatics tools to investigate potential functions and pathways of the associated
344 genes. We first employed DEPICT[49] to perform a gene set enrichment analysis, a tissue type enrichment,
345 and a gene prioritization analysis, on all variants with P value $< 1.00 \times 10^{-5}$ from Stage 3. The gene set
346 enrichment analysis resulted in 66 reconstituted gene sets, of which 55 (83%) were eye-related. To reduce
347 redundancies between pathways, we clustered the significant pathways into 13 meta gene sets (false
348 discovery rate (FDR) < 5% and a P value < 0.05) (Supplementary Methods 1, Figure 4, Supplementary
349 Excel File 4). The most significant gene set was the 'abnormal photoreceptor inner segment morphology'
350 (MP:0003730; P value = 1.79×10^{-7}). The eye-related meta gene sets consisted of the 'thin retinal outer
351 nuclear layer' (MP:0008515; 27 (55%) gene sets), 'detection of light stimulus' (GO:0009583; 13 (24%)
352 gene sets), 'nonmotile primary cilium' (GO:0031513; 4 (6%) gene sets), and 'abnormal anterior eye
353 segment morphology' (MP:0005193; 4 (6%) gene sets). The first three meta gene sets had a Pearson's
354 correlation > 0.6. Interestingly, *RGR*, *RP1L1*, *RORB* and *GNB3* were present in all of these meta gene
355 sets. Retina was the most significant tissue of expression according to the tissue enrichment analysis (P
356 value = 1.11×10^{-4}, FDR <0.01). From the gene prioritization according to DEPICT, 7 genes were

357 highlighted as the most likely causal genes at *P* value < 7.62 x 10-6 and FDR <0.05: *ANO2, RP1L1,*

358 *GNB3, EDN2, RORB* and *CABP4*.

359 Next, we performed a canonical pathway analysis on all genes annotated to the variants of Stage

360 3 using Ingenuity Pathway Analysis (IPA; http://www.ingenuity.com/index.html). All genes were run

361 against the IPA database incorporating functional biological evidence on genomic and proteomic

362 expression based on regulation or binding studies. IPA identified "Glutamate Receptor Signaling" with

363 central player *Nf-kB* gene as the most significant pathway after correction for multiple testing (ratio of the

364 number of molecules 8.8% and Fisher's Exact test *P* value = 1.56 x 10^{-4}; Figure 5, Supplementary Figure

365 10).

366

367 From disease associated loci to biological mechanisms

368 We adapted the scoring scheme designed by Fritsche et al.[50] to highlight genes for which there is

369 biological plausibility for a role in eye growth. We used 10 equally rated categories (maximum score 10;

370 genes with score ≥ 5 Table 3; all genes Supplementary Excel File 5; Online Methods, Supplementary

371 Methods 1): internal replication of index genetic variants in the individual cohort GWAS (CREAM-ASN,

372 CREAM-EUR and 23andMe), evidence for an eQTL effect in at least four tissue or cell types, annotation

373 to altered genomic function, ocular phenotype in humans and in mice, expression in human adult and fetal

374 ocular tissue, the presence of genes in the gene set enrichment, the presence of genes in the prioritization

375 analysis of DEPICT, and the presence of genes in the top 5 canonical pathway analysis of IPA. Sixty-five

376 index variants replicated in two or more individual cohorts; we found evidence for seven genetic variants

377 with eQTL effects in multiple tissue types; nine exonic variants, of which seven predicted protein-

378 alterations (Supplementary Table 4); 27 RNA genes, six located in the 3' or 5'UTR (Supplementary Table

379 7, Supplementary Figure 11), 84 genes resulting in an ocular phenotype in humans (Supplementary Excel

380 File 6) and 28 in mice (Supplementary Excel File 7); 169/212 (79%) genes expressed in human ocular

381 tissue (Supplementary Methods 1, Supplementary Excel File 8); 42 genes identified by DEPICT at *P*

382 value < 5.4 x 10^{-4} and FDR < 0.05 and 45 genes contributed to the most significant canonical pathways of
383 IPA. Notably, 48 of the associated genes encode known drug targets (Supplementary Excel File 9).
384 The gene with the highest biological plausibility score (score = 8) was *GNB3*, a highly conserved
385 gene encoding a guanine nucleotide-binding protein expressed in rod and cone photoreceptors and ON-
386 bipolar cells[51]. *GNB3* participates in signal transduction through G-protein coupled receptors and
387 enhances the temporal accuracy of phototransduction and ON-center signaling in the retina[51]. As
388 described above, the index SNP harbors a missense variant associated with refractive errors. Non-
389 synonymous mutations within *GNB3* are known to cause syndromic congenital stationary night
390 blindness[52] in humans, progressive retinopathy and globe enlargement in chickens[51], and abnormal
391 development of the photoreceptor-bipolar synapse in knock-out mice[53,54].
392 Other genes highly ranked (score = 7) include *CYP26A1, GRIA4*, *RDH5*, *RORB* and *RGR*, all
393 previously associated with refractive error, and one newly identified gene: *EFEMP1*. *EFEMP1* encodes a
394 member of the fibulin family of extracellular matrix glycoproteins, and is found pan-ocularly including in
395 the inner nuclear layer and Bruch's membrane. Mutations in this gene lead to specific macular
396 dystrophies[55], while variants have also been shown to co-segregate with primary open-angle glaucoma[56]
397 and associate with optic disc cup area[57].
398 Several other genes from our analysis are noteworthy for their function. *CABP4*, a calcium
399 binding protein expressed in cone and rod photoreceptor cells, mediates Ca^{2+} influx and glutamate release
400 in the photoreceptor-bipolar synapse[58]. Mutations in this gene have been described in congenital cone-rod
401 synaptic disorder[59], a retinal dystrophy associated with nystagmus, photophobia, and, remarkably, high
402 hyperopia. *KCNMA1* encodes pore forming alpha subunits of Ca^{2+}-activated K^+ (BK) channels. These
403 channels regulate synaptic transmission exclusively in the rod pathway[60]. A striking function of the other
404 previously identified genes is retinoic acid signaling and metabolism[61-63]. *ANO2* is a Ca^{2+}-activated Cl^-
405 channel recently reported to regulate retinal pigment epithelial (RPE) cell volume in a light-dependent
406 manner[64]. *EDN2* is a potent vasoconstrictor that binds to two G-protein-coupled receptors, *EDNRA*, which
407 residesd on bipolar dendrites, and *EDNRB*, which is present on Mueller and horizontal cells. Both receptors

408 are also present on choroidal vessels[65], implying that the choroid as well as retinal cells are target sites for
409 this gene. *RP1L1* is expressed in cone and rod photoreceptors where it is involved in the maintenance of
410 microtubules in the connecting cilium[66]. Mutations in this gene cause dominant macular dystrophy and
411 retinitis pigmentosa[67]. We replicated two genes known to cause myopia in family studies. *FBN1* harbors
412 mutations causing with Marfan (OMIM #154700) and Weil Marchesani (OMIM #608328) syndrome;
413 *PTPRR* was one of the candidates in the MYP3 locus, which was found by linkage in families with high
414 myopia[68].

415 The location of rs7449443 (*P* value 3.58 x 10^{-8}) is notable as it resides in between *DRD1* and
416 *FLJ16171*. *DRD1* encodes dopamine receptor 1 and is known to modulate dopamine receptor 2-mediated
417 events[69,70]. The dopamine pathway has been implicated in myopia pathogenesis in many studies[69,71]. SNPs
418 in and near other genes involved in the dopamine pathway (dopamine receptors, synthesis, degradation,
419 and transporters)[72-74] did not reveal genome-wide significant associations (Supplementary Methods 2,
420 Supplementary Table 8; Supplementary Figure 12).

421 There were twenty-eight genetic variants in or near DNA structures transcribing RNA genes (non
422 coding RNA, linc RNAs, tRNAs, snoRNas, rRNAs). Notably, five were in the transcription region and
423 thirteen were in the vicinity (>0 kb and ≤ 50 kb) of start or end of the RNA gene transcription region.
424 They received low scores, since many have no reported function or disease association to date (Table 3,
425 Supplementary Excel File 10, Supplementary Figure 11, Supplementary Table 7). Our ranking of genes
426 based on functional information existing in the public domain does not necessarily represent the true
427 order of importance for refractive error pathogenesis. The observation that genes with strong statistical
428 association were distributed over all scores supports this concept. Nevertheless, this list may help to select
429 genes for subsequent functional studies.

430 Finally, integration of all aforementioned data with findings from literature allowed us to annotate
431 a large number of genes to ocular cell types (Figure 6). Remarkably, all cell types of the retina harbored
432 refractive error genes, as well as the RPE, vascular endothelium, and extracellular matrix.

433

434 **Genetic pleiotropy**

435 We performed a GWAS catalogue look up using FUMA to investigate overlap of genes with other
436 common traits (Supplementary Figure 13)[75]. Refractive error and hyperopia were replicated significantly
437 after correcting for multiple testing (adjusted *P* value 1.44×10^{-52} and 9.34×10^{-9}, respectively). We found
438 significant overlap with 74 other traits, of which height (adjusted *P* value 1.11×10^{-10}), obesity (adjusted
439 *P* value 1.38×10^{-10}), and BMI (adjusted *P* value 4.05×10^{-7}) were most important. Ocular traits
440 significantly associated were glaucoma (optic cup area, intraocular pressure; adjusted *P* values 2.69×10^{-5}
441 and 3.01×10^{-5}, respectively) and age-related macular degeneration (adjusted *P* value 1.27×10^{-3}).
442
443

444 # DISCUSSION

445 Myopia may become the leading cause of world blindness in the near future, a grim outlook for which
446 current counteractions are still insufficient[11,76]. To improve understanding of the genetic landscape and
447 biology of the refractive error trait, we conducted a large GWAS meta-analysis in 160,420 participants of
448 mixed ancestry and replicated in 95,505 participants. This led to the identification of 139 independent
449 susceptibility loci by single variant analysis and 22 additional loci through post-GWAS methods, a four-
450 fold increase in refractive error genes. The majority of annotated genes were found to be expressed in the
451 human posterior segment of the eye. Using in silico analysis, we identified significant biological
452 pathways, of which retinal cell physiology, light processing, and specifically glutamate receptor signaling
453 were the most prominent mechanisms. Our integrated bio-informatic approach highlighted known ocular
454 functionality for many genes.

455 To ensure robustness of our genetic associations, we included studies of various designs and
456 populations, sought replication in an independent cohort of significant sample size, and stringently
457 accounted for population stratification by performing genomic control at all stages of the meta-analysis[77].

458 With this approach, we internally replicated all loci from CREAM in 23andMe, and replicated a
459 considerable proportion of the 23andMe loci in CREAM. We combined studies with outcomes based on
460 actual refractive error measurements as well as on self-reported age-of-myopia-onset, and found the
461 direction-of-effect of the associated variants, as well as their effect size, to be remarkably consistent.
462 Combining two different outcome measures may appear unconventional, but age of onset and refractive
463 error have been shown to be very tightly correlated[11,28]. Each year of earlier onset leads to a higher degree
464 of myopia[78,79]. Moreover, the high genetic correlation of common SNPs between the two phenotypes
465 underscores their similarity. Most compelling evidence was provided by replication of 86% of the
466 discovered variants in the independent UKEV cohort which also used conventional refractive error
467 measurements. This robustness indicates that both phenotypic outcomes (SphE and AODM) can be used
468 to capture a shared source of genetic variation. In addition, we found trans-ethnic replication of
469 significant loci, and a high per-allele correlation of genetic effects of common variants in the Europeans
470 and Asians. Our findings support a largely shared genetic predisposition to refractive error and myopia in
471 the two ethnicities, although ancestry-specific allelic effects may exist. The low heritability estimate in
472 Asians may, in part, be explained by the low representation of this ethnicity in our study sample.
473 Alternatively, it may imply that environmental factors explain a greater proportion of the phenotypic risk
474 and recent rise in myopia prevalence in this ancestry group[80].

475 Limitations of our study were the possibility of false negative findings due to genomic control,
476 and underrepresentation of studies with Asian ancestry. Heterogeneity of observed effect estimates was
477 large for several associated variants, but not unexpected given the large number of collaborating studies
478 with varying methodology.

479 Although neurotransmission was already a suggested pathway in our previous studies[26,27], our
480 current pathway analyses provide more in depth insights into the retinal circuitry driving refractive error.
481 DEPICT identified 'thin retinal outer nuclear layer', 'detection of light stimulus', and 'nonmotile primary
482 cilium' as the most important meta-gene sets. These are the main characteristics of photoreceptors, which
483 are located in the outer retina and contain cilia. These photosensitive cells drive the phototransduction

484 cascade in response to light, which in turn induces visual information processing. IPA pointed towards
485 glutamate receptor signaling as the most significant pathway. Glutamate is released by photoreceptors and
486 determines conductance of retinal signaling to the ON and OFF bipolar cells[81]. Our functional gene look
487 ups provide evidence that rod as well as cone bipolar cells play a role (rod: *CLU*; cone: *GNB3*). Taken
488 together, these findings strongly suggest that light response and light processing in the retina are initiating
489 factors leading to refractive error.

490 The genetic association with light dependent pathways may also link to the well-established
491 protective effect of outdoor exposure on myopia. We found suggestive evidence for a genetic association
492 with *DRD1,* the dopamine receptor D1 gene. The dopaminergic pathway has been studied extensively in
493 animal models for its role in controlling eye growth in response to light[69,71,82-91]. *DRD1* was found to be a
494 mediator in this process, as bright light increased DRD1 activity in the bipolar ON-pathway, and
495 diminished form deprivation myopia in mice. Blockage of DRD1 reversed this inhibitory effect[92]. We did
496 not find evidence for direct involvement of other genes in the dopamine pathway, but *GNB3* may be an
497 indirect modifier as it is a downstream signaling molecule of dopamine and has been shown to influence
498 availability of the dopamine transporter DAT[93]. Although a promising target for therapy, further evidence
499 of *DRD1* in human myopiagenesis is warranted.

500 Novel pathways elicited by the newly identified genes are anterior segment morphology
501 *(TCF7L2, VIPR2, MAF*) and angiogenesis (*FLT1*). In addition, the high number of variants residing near
502 small RNA genes suggests that post-transcriptional regulation is an important mechanism, as these RNAs
503 are known to play a distinct and central regulatory role in cells[94]. These findings will serve as leads for
504 future studies performing detailed mapping of cellular networks, and functional studies into genes
505 implicated in ocular phenotypes, harboring protein-altering variants, and proven drug targets.

506 Our evaluation of shared genetics between refractive error and other disease-relevant phenotypes
507 highlighted overlap with anthropometric traits such as height, obesity, and BMI. This could give valuable
508 additional clues as to the phenotypic outcomes of perturbations of some of the networks identified.

509 Our genetic observations add credence to the current notion that refractive errors are caused by a
510 retina-to-sclera signaling cascade that induces scleral remodeling in response to light stimuli. The concept
511 of this cascade originates from various animal models showing that form deprivation, retinal defocus and
512 contrast, ambient light, and wavelength can influence eye growth in young animals[95-97]. Cell-specific
513 moieties in this putative signaling cascade in humans were largely unknown, although animal models
514 implicated GABA, dopamine, all-trans-retinoic acid and TGF-β[69,91,98,99]. Our study provides a large
515 number of new molecular candidates for this cascade, and clearly shows that a wide range of neuronal cell
516 types in the retina, the RPE, the vascular endothelium, as well as components of the extracellular matrix
517 are implicated (Figure 6). The many interprotein relationships (Figure 4) exemplify the complexity of eye
518 growth, and provide a challenge to develop strategies to prevent pathological eye elongation.

519 In conclusion, by using a cross-ancestry design in the largest study population on common
520 refractive errors to date, we uncovered numerous novel loci and pathways involved in eye growth. Our
521 multi-disciplinary approach incorporating GWAS data with *in silico* analyses and expression experiments
522 provides an example for the design of future genetic studies for complex traits. Additional genetic insights
523 into refractive errors will be gained by increasing sample size, greater genotyping depth, family studies
524 for identifying rare alleles of large effect, and by evaluating population extremes. Our list of plausible
525 genes and pathways provide a plethora of data for future studies focusing on gene-environment
526 interaction, and on translation of GWAS findings into starting points for therapy.

527

528

529 # ONLINE METHODS

530 ## Ethics Statement

531 All human research was approved by the relevant institutional review boards and conducted according to
532 the Declaration of Helsinki. All CREAM participants provided written informed consent; all 23andMe
533 applicants provided informed consent online, and answered surveys according to 23andMe's human
534 subjects protocol, which was reviewed and approved by Ethical & Independent Review Services, an
535 AAHRPP-accredited institutional review board.

536 ## Study data

537 The study populations were participants of the Consortium for Refractive Error and Myopia (CREAM)
538 comprising of 41,793 individuals with European ancestry from 26 cohorts (CREAM-EUR) and 11,935
539 individuals with Asian ancestry from 8 studies (CREAM-ASN); and customers of the 23andMe genetic
540 testing company who gave informed consent for inclusion in research studies consisting of 104,293
541 individuals (2 cohorts of individuals with European ancestry, $N = 12,128$ and $N = 92,165$, respectively).
542 All participants included in this analysis from CREAM and 23andMe were aged 25 years or older.
543 Participants with conditions that could alter refraction, such as cataract surgery, laser
544 refractive procedures, retinal detachment surgery, keratoconus as well as ocular or systemic syndromes
545 were excluded from the analyses. Recruitment and ascertainment strategies varied per study
546 (Supplementary Table 1a,b, and Supplementary Methods 3). Refractive error represented by
547 measurements of refraction and analyzed as spherical equivalent (SphE =spherical refractive error + 1/2
548 cylinder refractive error) was the outcome variable for CREAM; myopic refractive error represented by
549 self-reported age of diagnosis of myopia (AODM) for 23andMe[27].

550

551 ## Genotype calling and imputation

552 Samples were genotyped on different platforms and study specific quality control measures of the
553 genotyped variants were implemented before association analysis (Supplementary Table 1a). Genotypes
554 were imputed using the appropriate ancestry-matched reference panel for all cohorts from the 1000
555 Genomes Project (Phase I version 3, March 2012 release) with either minimac[100] or IMPUTE[101,102]. The
556 metrics for pre-imputation quality control varied amongst studies, but genotype call rate thresholds were
557 set at high level (≥0.95 for both CREAM and 23andMe). These metrics were similar to our previous
558 GWAS analyses[26,27]; details per cohort can be found in Supplementary Table 1a.

559 ## GWAS per study

560 For each CREAM cohort, a single marker analysis for the SphE (in diopters) phenotype was carried out
561 using linear regression adjusting for age, sex and up to the first five principal components. All non-
562 family-based cohorts removed one of each pair of relatives (after detection using either GCTA or
563 IBS/IBD analysis). In family-based cohorts, a score test-based association was used to adjust for within-
564 family relatedness[103,104]. For the 23andMe participants, Cox proportional hazards analysis testing AODM
565 as the dependent variable were performed as previously described[27], with P values calculated using a
566 likelihood ratio test for the single marker genotype term. We used an additive SNP allelic effect model for
567 all analyses.

568

569 ## Centralized quality control per study

570 After individual GWAS, all studies underwent a second round of quality control (QC). Quantile-quantile,
571 effect allele frequency, $P – Z$ test, standard error – sample size, and genomic control inflation factor plots
572 were generated for each individual cohort using EasyQC[105] (Supplementary Figure 2.1, 2.2, 2.3) . All
573 analytical issues discovered during this QC step were resolved per individual cohort.

574

GWAS meta-analyses

The GWAS meta-analyses were performed in three stages (Supplementary Figure 1). In Stage 1, European (CREAM-EUR) and Asian (CREAM-ASN) participants from the CREAM cohort were meta-analysed separately. Subsequently, all CREAM cohorts (CREAM-ALL) were meta-analysed. Variants with MAF < 1% or imputation quality score < 0.3 (info metric of IMPUTE) or Rsq < 0.3 (minimac) were excluded. A fixed effects inverse variance-weighted meta-analysis was performed using METAL[106]. In all stages, each genetic variant had to be represented by at least half of the entire study population and at least represented by 13 cohorts in CREAM and one cohort in 23andMe. For SNPs with high heterogeneity (at $P < 0.05$), we also performed a random effects meta-analysis using METASOFT[50]. In Stage 2, a meta-analysis of the two 23andMe cohorts was performed, using similar filtering but a lower MAF threshold (< 0.5%). In Stage 3, CREAM-ALL and 23andMe samples were combined using a fixed effects meta-analysis based on *P* values and direction of effect.

In Stage 3, we chose a different weighting scheme due to the differences in effect size scaling; 23andMe used a less accurate phenotype variable (AODM); i.e. the *effective* sample size of the 23andMe was approximately equivalent to the *effective* sample size of CREAM-ALL (Figure 2b), thus weighting by ($1/\sqrt{n_{effective}}$) yielded a final weighting ratio of 1:1[107,108]. Genome-wide statistical significance was defined at $P < 5.0 \times 10^{-8}$ [109]. All three meta-analysis stages were performed under genomic control. Study specific and meta-analysis lambda (λ) estimates are shown in Supplementary Figure 7; to check for confounding biases (e.g. cryptic relatedness and population stratification), LD score intercepts from LD score regressions per ancestry were constructed (Supplementary Figure 8)[30]. To check the robustness of signals, we performed a conventional random effects models using METASOFT, fixed effects models weighted on sample size and on weights estimated from standard error per allele tested using METAL (Supplementary Excel Files 1 and Supplementary Excel Files 2).

Manhattan (modified version of package 'qqman'), regional, box, and forest plots were made using R version 3.2.3 and LocusZoom[110]. An overview of the Hardy Weinberg *P* values of all index variants per

600 cohort can be found in Supplementary Excel File 3. The comparison between refractive error and age-of-
601 onset was performed using the LDSC program[30].
602

603 Population stratification and heritability calculations

604 Each study assessed the degree of genetic admixture and stratification in their study participants through
605 the use of principal components. Homogeneity of participants was assured by removal of all individuals
606 whose ancestry did not match the prevailing ancestral group. We used genomic inflation factors to control
607 for admixture and stratification, and performed genomic-controlled meta-analysis to account for the
608 effects of any residual heterogeneity. To further distinguish between inflation from a true polygenic signal
609 and population stratification, we examined the relationship between test statistics and linkage
610 disequilibrium (LD) with LDSC. CREAM-EUR, CREAM-ASN and 23andMe were evaluated separately;
611 variants not present in HapMap3 and MAF < 1% were excluded. SNP heritability estimates were
612 calculated using LDSC for the same set of genetic variants.

613 Locus definition and annotation

614 All study effect size estimates were oriented to the positive strand of the NCBI Build 37 reference
615 sequence of the human genome. The index variant of a locus was defined as the variant with the lowest *P*
616 value in a region spanning a 100 kb window of the most outer genome wide significant variant of that
617 same region. We annotated all index variants using the web-based version of ANNOVAR[111]based on
618 UCSC Known Gene Database[35]. For variants within the coding sequence or 5' or 3' untranslated regions
619 of a gene, that gene was assigned to the index variant (note that this led to more than 1 gene being
620 assigned to variants located within the transcription units of multiple, overlapping genes). For variants in
621 intergenic regions, the nearest 5' gene and the nearest 3' gene were assigned to the variant. Index variants
622 were annotated to functional RNA elements when described as such in the UCSC Known Gene Database.

623 We used conservation (PhyloP[112]) and prediction tools (SIFT[39], Mutation Taster[113], align GVGD[40,41],
624 PolyPhen-2[36]) to predict the pathogenicity of protein-altering exonic variants.
625

626 Conditional signal analysis

627
628 We performed conditional analysis to identify additional independent signals nearby the index variant at
629 each locus, using GCTA-COJO[32]. We transformed the Z-scores of the summary statistics to beta's using
630 the following formula: Standard Error = $\sqrt{1/2 * N * MAF(1-MAF)}$. We performed the GCTA-COJO
631 analysis[32], utilizing summary-level statistics from the meta-analysis on all cohorts. Linkage
632 disequilibrium (LD) between variants was estimated from the Rotterdam Study I-III.
633

634 Replication in UK Biobank

635 The UK Biobank Eye & Vision (UKEV) Consortium performed a GWAS of refractive error in 95,505
636 participants of European ancestry aged 37-73 year with no history of eye disorders[33]. Refractive error was
637 measured using an autorefractor; SphE was calculated per eye and averaged between the two eyes. To
638 account for relatedness a mixed model analysis with BOLT-LMM was used[114], including age, gender,
639 genotyping array, and the first 10 principal components as covariates. Analysis was restricted to markers
640 present on the HRC reference panel[115]. We performed lookups for all independent genetic variants
641 identified in our Stage 3 meta-analysis and conditional analysis. For variants not present in UKEV, we
642 performed lookups for a surrogate variant in high LD (r^2 >0.8). When more than one potential surrogate
643 variant was available, the variant in strongest LD with the index variant was selected.
644

645 Post-GWAS analyses

646 We performed two gene-based tests to identify additional significant genes not found in the single variant
647 analysis. First, we applied the gene-based test implemented in fastBAT[42] to the per-variant summary
648 statistics of the meta-analysis of all European cohorts (23andMe and CREAM-EUR). We used the default

649 parameters (all variants in or within 50kb of a gene) and focused on variants with a gene-based *P* value
650 <2 x 10^{-6} (Bonferroni correction based on 25,000 genes) and the per-variant *P* value >5 x 10^{-8}. Secondly,
651 we applied another gene-based test in EUGENE[43] which only includes variants which are eQTLs (GTex,
652 blood[116]). EUGENE tests an hypothesis predicated on eQTLs as key drivers of the association signal.
653 eQTLs within 50kb of a gene were included in the test. Genes with EUGENE *P* value <2 x 10^{-6} (and not
654 found in the single variant analysis) were considered to be significant. Finally, we used functional
655 annotation information from genome-wide significant loci to reweigh results using fgwas (version
656 0.3.64[44]). This approach is able to identify risk loci that otherwise might not reach the genome-wide
657 significance threshold in standard GWAS. Details about this approach can be found in Supplementary
658 Methods 4.

659

660 ## Refractive errors and myopia risk prediction

661 To assess the risk of the entire range of refractive errors, we computed polygenic risk scores (PGRS) for
662 the population-based Rotterdam Studies (RS) I, RS-II and RS-III using the *P* values and *Z* scores from a
663 meta-analysis on CREAM-ALL and 23andMe, excluding the RS I-III cohorts. Only variants with high
664 imputation quality (IMPUTE info score > 0.5 or minimac Rsq > 0.8) and MAF > 1% were considered. *P*
665 value-based clumping was performed with PLINK[117], using an r^2 threshold of 0.2 and a physical distance
666 threshold of 500 kb, excluding the MHC region. This resulted in a total of 243,938 variants. For each
667 individual in RS-I, RS-II and RS-III (*N* = 10,792), PGRS were calculated using the --score command in
668 PLINK across strata of *P* value thresholds: 5.0 x 10^{-8}, 5.0 x 10^{-7}, 5.0 x 10^{-6}, 5.0 x 10^{-5}, 5.0 x 10^{-4}, 0.005,
669 0.01, 0.05, 0.1, 0.5, 0.8 and 1.0. The proportion of variance explained by each PGRS model was
670 calculated as the difference in the R^2 between two regression models; one where SphE was regressed on
671 age, sex, the first five principal components, and the other also including the PGRS as an additional

672 covariate. Subsequently, AUCs were calculated for myopia (SphE ≤ -3 SD) versus hyperopia (SphE ≥ +3
673 SD).
674

675 Genetic correlation between ancestries

676 We used Popcorn[48] to investigate ancestry-related differences in the genetic architecture of refractive
677 error and myopia. Pairwise analyses were carried out using the GWAS summary statistics from 23andMe
678 (N = 104,292), CREAM-EUR (N = 44,192) and CREAM-EAS (N = 9,826) meta-analyses. Only SNPs
679 with MAF ≥ 5% were included, resulting in a final set of 3,625,602 SNPs for analyses involving
680 23andMe and 3,642,928 SNPs for the CREAM-EUR versus CREAM-EAS analysis. Reference panels
681 were constructed using genotype data from 503 European and 504 East Asian individuals sequenced as
682 part of the 1000 Genomes Project (release 2013-05-02 downloaded from: ftp.1000genomes.ebi.ac.uk).
683 The reference panel VCF files were filtered using PLINK[117] to remove indels, strand-ambiguous variants,
684 variants without an "rs" id prefix, and variants located in the MHC region on chromosome 6
685 (chr6:25,000,000-33,500,000; Build 37).
686

687 Analysis between phenotypes

688 To evaluate consistency of genotypic effects across studies that employed different phenotype definitions,
689 we compared effect sizes from GWAS studies of either SphE or AODM in Europeans, i.e. CREAM-EUR
690 (N = 44,192) or 23andMe (N = 104,293) respectively. Marker-wise additive genetic effect sizes (in units
691 diopters per copy of the risk allele) for SphE were compared against those (in units log(HR) per copy of
692 the risk allele) for AODM. Data was visualised using R. Genetic correlation between the two phenotypes
693 SphE and AODM was calculated using LD score regression. This analysis included all common SNPs
694 (MAF > 0.01) present in HapMap3.
695

696 Evidence for functional involvement

697 In order to rank genes according to biological plausibility, we scored annotated genes based on our own
698 findings and published reports for a potential functional role in refractive error. Points were assigned for
699 each gene on the basis of 10 categories (details on the methodology per category are provided in
700 Supplementary Methods 3): internal replication of index genetic variants in the individual cohort GWAS
701 analyses through Bonferroni corrections (CREAM-ASN, CREAM-EUR and 23andMe; *pBonferroni* 1.10
702 x 10^{-4}), evidence for eQTL using the FUMA[32] and extensive look-ups in GtEx, evidence of expression in
703 the eye in developmental and adult ocular tissues, presence of an eye phenotype in knock-out mice (MGI
704 and IMPC database), presence of an eye phenotype in humans (OMIM[118] (http://omim.org),
705 DisGeNET[119]), location in a functional region of a gene (wANNOVAR), presence of the gene in a
706 significant enriched functional pathway with false discovery rate < 0.05 (DEPICT[49]), presence of the gene
707 in the gene priority analysis of DEPICT with false discovery rate < 0.05 and the presence of the gene in
708 the canonical pathway analysis of Ingenuity Pathway Analysis (IPA;
709 http://www.ingenuity.com/index.html). Furthermore, we performed a systematic search for each gene to
710 assess its potential as a drug target (SuperTarget[120], STITCH[121], DrugBank[122], PharmaGkb[123]). All
711 information derived from this study and literature were used to annotate genes to retinal cell types.
712

713 Genetic pleiotropy

714 To investigate overlap of genes with other common traits, we performed a look-up in the GWAS catalog
715 using FUMA. Multiple testing correction (i.e. Benjamini-Hochberg) was performed. Traits were
716 significantly associated when adjusted *P* value ≤ 0.05 and the number of genes that overlap with the
717 GWAS catalog gene sets was ≥ 2.
718

719 Data availability statement

720 The summary statistics of the Stage 3 meta-analysis are included in supplementary information files of
721 this published article. In order to protect the privacy of the participants in our cohorts, further summary
722 statistics of Stage 1 (CREAM) and Stage 2 (23andMe) will be available upon request. Please contact

723 c.c.w.klaver@erasmusmc.nl (CREAM) and/or apply.research@23andMe.com (23andMe) for more

724 information and to access the data.

725

726 **Acknowledgments**

727 We gratefully thank the invaluable contributions of all study participants, their relatives and staff at the

728 recruitment centers. Complete funding information and acknowledgments by study can be found in the

729 **Supplementary Note**.

730

731

732 **Author contributions**

733 M.S.T., V.J.M.V., S.M., J.A.G., A.I.I.G., R.W., P.G.H., A.I.I.G., and E.M.v.L. performed the analyses.
734 C.C.W.K., V.J.M.V., M.S.T., R.W., J.A.G., and S.M. drafted the manuscript, and C.J.H., P.G.H., A.P.K.,
735 C.M.v.D., D.S, E.M.v.L., J.E.B.W., J.T., N.A.F., Q.F., S.M.S., and V.V. critically reviewed the
736 manuscript. A.N., A.P.K., A.T., C.B., C.Gi., C.L.S., C.Y.C., G.Bi., G.C., I.R., J.E.B.W., J.E.H., J.S.Ri.,
737 J.W., J.X., K.M.W., K.Y., M.P.C., M.S.H., M.S.T., N.A.F., N.E., P.C., P.Gh., P.K.J., Q.F., R.Ho., R.L.S.,
738 R.P.I., R.W., T.H., T.H.S.A., T.Z., V.V., W.Y.S., W.Z., X.L.S., Y.C.H., Y.S., and Y.Y.T. performed data
739 analysis for the individual studies; and A.D.P., A.G.U., A.T., A.W.H., B.E.K.K., C.C.W.K., C.D., C.H.,
740 C.J.H., C.W., C.Y.C., D.A.M., F.R., G.Be., H.M.H., J.A.G., J.B.J., J.E.B.W., J.E.C., J.F.W., J.H.L.,
741 J.R.V., J.S.Ra., J.S.Ri., J.T., K.Y., M.A.M.S., N.G.M., N.P., O.Po., O.Pa., O.T.R., P.Gu., P.J.F., P.M.,
742 P.N.B., R.K., S.K.I., S.M.S., T.L., T.M., W.Z., Y.C.H., and Y.X.W. contributed to data assembly.
743 A.A.B.B., A.W., C.Gr., D.S., K.N.W., S.W.J.T., and T.Y. performed expression experiments, and M.S.T.,
744 A.A.B.B., P.J.v.d.S., and R.Ha. performed in silico pathway analyses. C.C.W.K. and C.J.H. conceived
745 and designed the outline of the current report, and jointly with A.M., A.H., A.W.H., C.D., C.H., C.J.H.,
746 C.M.v.D., C.W., C.Y.C., D.A.M., D.S., E.S.T., F.M., G.Bi., I.R., J.A.G., J.B.J., J.E.B.W., J.E.C., J.F.W.,
747 J.H.L., J.R.V., J.T., N.A., N.A.F., N.P., O.Pa., O.T.R., P.J.F., P.N.B., S.K.I., S.M.S., T.L., T.Y.W., T.Y.,
748 V.V., Y.X.W., and Y.Y.T. supervised conduction of experiments and analyses.
749

750 **References**

751

752 1. Pan, C.W., Ramamurthy, D. & Saw, S.M. Worldwide prevalence and risk factors for myopia.
753 *Ophthalmic Physiol Opt* **32**, 3-16 (2012).
754 2. Morgan, I.G. What Public Policies Should Be Developed to Deal with the Epidemic of Myopia?
755 *Optom Vis Sci* **93**, 1058-60 (2016).
756 3. Morgan, I. & Rose, K. How genetic is school myopia? *Prog Retin Eye Res* **24**, 1-38 (2005).
757 4. Morgan, I.G., Ohno-Matsui, K. & Saw, S.M. Myopia. *Lancet* **379**, 1739-48 (2012).
758 5. Williams, K.M. *et al.* Increasing Prevalence of Myopia in Europe and the Impact of Education.
759 *Ophthalmology* **122**, 1489-97 (2015).
760 6. Williams, K.M. *et al.* Prevalence of refractive error in Europe: the European Eye Epidemiology
761 (E(3)) Consortium. *Eur J Epidemiol* **30**, 305-15 (2015).
762 7. Vongphanit, J., Mitchell, P. & Wang, J.J. Prevalence and progression of myopic retinopathy in an
763 older population. *Ophthalmology* **109**, 704-11 (2002).
764 8. Seet, B. *et al.* Myopia in Singapore: taking a public health approach. *Br J Ophthalmol* **85**, 521-6
765 (2001).
766 9. Smith, T.S., Frick, K.D., Holden, B.A., Fricke, T.R. & Naidoo, K.S. Potential lost productivity
767 resulting from the global burden of uncorrected refractive error. *Bull World Health Organ* **87**,
768 431-7 (2009).
769 10. Verhoeven, V.J. *et al.* Visual consequences of refractive errors in the general population.
770 *Ophthalmology* **122**, 101-9 (2015).
771 11. Tideman, J.W. *et al.* Association of Axial Length With Risk of Uncorrectable Visual Impairment
772 for Europeans With Myopia. *JAMA Ophthalmol* **134**, 1355-1363 (2016).
773 12. Flitcroft, D.I. The complex interactions of retinal, optical and environmental factors in myopia
774 aetiology. *Prog Retin Eye Res* **31**, 622-60 (2012).
775 13. Nakanishi, H. *et al.* A genome-wide association analysis identified a novel susceptible locus for
776 pathological myopia at 11q24.1. *PLoS Genet* **5**, e1000660 (2009).
777 14. Lam, C.Y. *et al.* A genome-wide scan maps a novel high myopia locus to 5p15. *Invest*
778 *Ophthalmol Vis Sci* **49**, 3768-78 (2008).
779 15. Stambolian, D. *et al.* Meta-analysis of genome-wide association studies in five cohorts reveals
780 common variants in RBFOX1, a regulator of tissue-specific splicing, associated with refractive
781 error. *Hum Mol Genet* **22**, 2754-64 (2013).
782 16. Fan, Q. *et al.* Genetic variants on chromosome 1q41 influence ocular axial length and high
783 myopia. *PLoS Genet* **8**, e1002753 (2012).
784 17. Fan, Q. *et al.* Meta-analysis of gene-environment-wide association scans accounting for education
785 level identifies additional loci for refractive error. *Nat Commun* **7**, 11008 (2016).
786 18. Cheng, C.Y. *et al.* Nine Loci for Ocular Axial Length Identified through Genome-wide
787 Association Studies, Including Shared Loci with Refractive Error. *Am J Hum Genet* **93**, 264-77
788 (2013).
789 19. Shi, Y. *et al.* Exome sequencing identifies ZNF644 mutations in high myopia. *PLoS Genet* **7**,
790 e1002084 (2011).
791 20. Shi, Y. *et al.* Genetic variants at 13q12.12 are associated with high myopia in the Han Chinese
792 population. *Am J Hum Genet* **88**, 805-13 (2011).
793 21. Li, Y.J. *et al.* Genome-wide association studies reveal genetic variants in CTNND2 for high
794 myopia in Singapore Chinese. *Ophthalmology* **118**, 368-75 (2011).
795 22. Li, Z. *et al.* A genome-wide association study reveals association between common variants in an
796 intergenic region of 4q25 and high-grade myopia in the Chinese Han population. *Hum Mol Genet*
797 **20**, 2861-8 (2011).
798 23. Liu, J. & Zhang, H.X. Polymorphism in the 11q24.1 genomic region is associated with myopia: a
799 comprehensive genetic study in Chinese and Japanese populations. *Mol Vis* **20**, 352-8 (2014).

800 24. Tran-Viet, K.N. *et al.* Mutations in SCO2 are associated with autosomal-dominant high-grade
801 myopia. *Am J Hum Genet* **92**, 820-6 (2013).
802 25. Aldahmesh, M.A. *et al.* Mutations in LRPAP1 are associated with severe myopia in humans. *Am*
803 *J Hum Genet* **93**, 313-20 (2013).
804 26. Verhoeven, V.J. *et al.* Genome-wide meta-analyses of multiancestry cohorts identify multiple
805 new susceptibility loci for refractive error and myopia. *Nat Genet* (2013).
806 27. Kiefer, A.K. *et al.* Genome-wide analysis points to roles for extracellular matrix remodeling, the
807 visual cycle, and neuronal development in myopia. *PLoS Genet* **9**, e1003299 (2013).
808 28. Wojciechowski, R. & Hysi, P.G. Focusing in on the complex genetics of myopia. *PLoS Genet* **9**,
809 e1003442 (2013).
810 29. Genomes Project, C. *et al.* A global reference for human genetic variation. *Nature* **526**, 68-74
811 (2015).
812 30. Bulik-Sullivan, B.K. *et al.* LD Score regression distinguishes confounding from polygenicity in
813 genome-wide association studies. *Nat Genet* **47**, 291-5 (2015).
814 31. Yang, J. *et al.* Genomic inflation factors under polygenic inheritance. *Eur J Hum Genet* **19**, 807-
815 12 (2011).
816 32. Watanabe, K., Taskesen, E., van Bochoven, A. & Posthuma, D. FUMA: Functional mapping and
817 annotation of genetic associations. *bioRxiv* (2017).
818 33. Plotnikov, D., Guggenheim, J. & Is a large eye size a risk factor for myopia? A Mendelian
819 randomization study. *bioRxiv* (2017).
820 34. UCSC Genome Browser.
821 35. Hsu, F. *et al.* The UCSC Known Genes. *Bioinformatics* **22**, 1036-46 (2006).
822 36. Adzhubei, I.A. *et al.* A method and server for predicting damaging missense mutations. *Nat*
823 *Methods* **7**, 248-9 (2010).
824 37. Ng, P.C. & Henikoff, S. SIFT: Predicting amino acid changes that affect protein function. *Nucleic*
825 *Acids Res* **31**, 3812-4 (2003).
826 38. Kelly, M.P. Does phosphodiesterase 11A (PDE11A) hold promise as a future therapeutic target?
827 *Curr Pharm Des* **21**, 389-416 (2015).
828 39. Kumar, P., Henikoff, S. & Ng, P.C. Predicting the effects of coding non-synonymous variants on
829 protein function using the SIFT algorithm. *Nat Protoc* **4**, 1073-81 (2009).
830 40. Mathe, E. *et al.* Computational approaches for predicting the biological effect of p53 missense
831 mutations: a comparison of three sequence analysis based methods. *Nucleic Acids Res* **34**, 1317-
832 25 (2006).
833 41. Tavtigian, S.V. *et al.* Comprehensive statistical study of 452 BRCA1 missense substitutions with
834 classification of eight recurrent substitutions as neutral. *J Med Genet* **43**, 295-305 (2006).
835 42. Bakshi, A. *et al.* Fast set-based association analysis using summary data from GWAS identifies
836 novel gene loci for human complex traits. *Sci Rep* **6**, 32894 (2016).
837 43. Ferreira, M.A. *et al.* Gene-based analysis of regulatory variants identifies 4 putative novel asthma
838 risk genes related to nucleotide synthesis and signaling. *J Allergy Clin Immunol* (2016).
839 44. Pickrell, J.K. Joint analysis of functional genomic data and genome-wide association studies of
840 18 human traits. *Am J Hum Genet* **94**, 559-73 (2014).
841 45. International Schizophrenia, C. *et al.* Common polygenic variation contributes to risk of
842 schizophrenia and bipolar disorder. *Nature* **460**, 748-52 (2009).
843 46. Verhoeven, V.J. *et al.* Large scale international replication and meta-analysis study confirms
844 association of the 15q14 locus with myopia. The CREAM consortium. *Hum Genet* **131**, 1467-80
845 (2012).
846 47. Finucane, H.K. *et al.* Partitioning heritability by functional annotation using genome-wide
847 association summary statistics. *Nat Genet* **47**, 1228-35 (2015).
848 48. Brown, B.C., Asian Genetic Epidemiology Network Type 2 Diabetes, C., Ye, C.J., Price, A.L. &
849 Zaitlen, N. Transethnic Genetic-Correlation Estimates from Summary Statistics. *Am J Hum Genet*
850 **99**, 76-88 (2016).

851 49. Pers, T.H. *et al.* Biological interpretation of genome-wide association studies using predicted
852 gene functions. *Nat Commun* **6**, 5890 (2015).
853 50. Fritsche, L.G. *et al.* A large genome-wide association study of age-related macular degeneration
854 highlights contributions of rare and common variants. *Nat Genet* **48**, 134-43 (2016).
855 51. Ritchey, E.R. *et al.* Vision-guided ocular growth in a mutant chicken model with diminished
856 visual acuity. *Exp Eye Res* **102**, 59-69 (2012).
857 52. Vincent, A. *et al.* Biallelic Mutations in GNB3 Cause a Unique Form of Autosomal-Recessive
858 Congenital Stationary Night Blindness. *Am J Hum Genet* **98**, 1011-9 (2016).
859 53. Blake, J.A. *et al.* Mouse Genome Database (MGD)-2017: community knowledge resource for the
860 laboratory mouse. *Nucleic Acids Res* **45**, D723-D729 (2017).
861 54. Nikonov, S.S. *et al.* Cones respond to light in the absence of transducin beta subunit. *J Neurosci*
862 **33**, 5182-94 (2013).
863 55. Stone, E.M. *et al.* A single EFEMP1 mutation associated with both Malattia Leventinese and
864 Doyne honeycomb retinal dystrophy. *Nat Genet* **22**, 199-202 (1999).
865 56. Mackay, D.S., Bennett, T.M. & Shiels, A. Exome Sequencing Identifies a Missense Variant in
866 EFEMP1 Co-Segregating in a Family with Autosomal Dominant Primary Open-Angle Glaucoma.
867 *PLoS One* **10**, e0132529 (2015).
868 57. Springelkamp, H. *et al.* ARHGEF12 influences the risk of glaucoma by increasing intraocular
869 pressure. *Hum Mol Genet* **24**, 2689-99 (2015).
870 58. Haeseleer, F. *et al.* Essential role of Ca2+-binding protein 4, a Cav1.4 channel regulator, in
871 photoreceptor synaptic function. *Nat Neurosci* **7**, 1079-87 (2004).
872 59. Littink, K.W. *et al.* A novel homozygous nonsense mutation in CABP4 causes congenital cone-
873 rod synaptic disorder. *Invest Ophthalmol Vis Sci* **50**, 2344-50 (2009).
874 60. Grimes, W.N., Li, W., Chavez, A.E. & Diamond, J.S. BK channels modulate pre- and
875 postsynaptic signaling at reciprocal synapses in retina. *Nat Neurosci* **12**, 585-92 (2009).
876 61. Parker, R.O. & Crouch, R.K. Retinol dehydrogenases (RDHs) in the visual cycle. *Exp Eye Res*
877 **91**, 788-92 (2010).
878 62. Radu, R.A. *et al.* Retinal pigment epithelium-retinal G protein receptor-opsin mediates light-
879 dependent translocation of all-trans-retinyl esters for synthesis of visual chromophore in retinal
880 pigment epithelial cells. *J Biol Chem* **283**, 19730-8 (2008).
881 63. Luo, T., Sakai, Y., Wagner, E. & Drager, U.C. Retinoids, eye development, and maturation of
882 visual function. *J Neurobiol* **66**, 677-86 (2006).
883 64. Keckeis, S., Reichhart, N., Roubeix, C. & Strauss, O. Anoctamin2 (TMEM16B) forms the Ca2+-
884 activated Cl- channel in the retinal pigment epithelium. *Exp Eye Res* **154**, 139-150 (2016).
885 65. Prasanna, G., Narayan, S., Krishnamoorthy, R.R. & Yorio, T. Eyeing endothelins: a cellular
886 perspective. *Mol Cell Biochem* **253**, 71-88 (2003).
887 66. Yamashita, T. *et al.* Essential and synergistic roles of RP1 and RP1L1 in rod photoreceptor
888 axoneme and retinitis pigmentosa. *J Neurosci* **29**, 9748-60 (2009).
889 67. Davidson, A.E. *et al.* RP1L1 variants are associated with a spectrum of inherited retinal diseases
890 including retinitis pigmentosa and occult macular dystrophy. *Hum Mutat* **34**, 506-14 (2013).
891 68. Hawthorne, F. *et al.* Association mapping of the high-grade myopia MYP3 locus reveals novel
892 candidates UHRF1BP1L, PTPRR, and PPFIA2. *Invest Ophthalmol Vis Sci* **54**, 2076-86 (2013).
893 69. Feldkaemper, M. & Schaeffel, F. An updated view on the role of dopamine in myopia. *Exp Eye*
894 *Res* **114**, 106-19 (2013).
895 70. Paul, M.L., Graybiel, A.M., David, J.C. & Robertson, H.A. D1-like and D2-like dopamine
896 receptors synergistically activate rotation and c-fos expression in the dopamine-depleted striatum
897 in a rat model of Parkinson's disease. *J Neurosci* **12**, 3729-42 (1992).
898 71. Stone, R.A., Lin, T., Laties, A.M. & Iuvone, P.M. Retinal dopamine and form-deprivation
899 myopia. *Proc Natl Acad Sci U S A* **86**, 704-6 (1989).

900 72. Gardner, M., Bertranpetit, J. & Comas, D. Worldwide genetic variation in dopamine and
901 serotonin pathway genes: implications for association studies. *Am J Med Genet B Neuropsychiatr*
902 *Genet* **147B**, 1070-5 (2008).
903 73. D'Souza, U.M. & Craig, I.W. Functional polymorphisms in dopamine and serotonin pathway
904 genes. *Hum Mutat* **27**, 1-13 (2006).
905 74. Beaulieu, J.M. & Gainetdinov, R.R. The physiology, signaling, and pharmacology of dopamine
906 receptors. *Pharmacol Rev* **63**, 182-217 (2011).
907 75. MacArthur, J. *et al.* The new NHGRI-EBI Catalog of published genome-wide association studies
908 (GWAS Catalog). *Nucleic Acids Res* **45**, D896-D901 (2017).
909 76. Holden, B.A. *et al.* Global Prevalence of Myopia and High Myopia and Temporal Trends from
910 2000 through 2050. *Ophthalmology* **123**, 1036-42 (2016).
911 77. Cardon, L.R. & Palmer, L.J. Population stratification and spurious allelic association. *Lancet* **361**,
912 598-604 (2003).
913 78. Chua, S.Y. *et al.* Age of onset of myopia predicts risk of high myopia in later childhood in
914 myopic Singapore children. *Ophthalmic Physiol Opt* **36**, 388-94 (2016).
915 79. Williams, K.M. *et al.* Age of myopia onset in a British population-based twin cohort. *Ophthalmic*
916 *Physiol Opt* **33**, 339-45 (2013).
917 80. Dolgin, E. The myopia boom. *Nature* **519**, 276-8 (2015).
918 81. Connaughton, V. Glutamate and Glutamate Receptors in the Vertebrate Retina. in *Webvision: The*
919 *Organization of the Retina and Visual System* (eds. Kolb, H., Fernandez, E. & Nelson, R.) (Salt
920 Lake City (UT), 1995).
921 82. Hung, G.K., Mahadas, K. & Mohammad, F. Eye growth and myopia development: Unifying
922 theory and Matlab model. *Comput Biol Med* **70**, 106-18 (2016).
923 83. Norton, T.T. What Do Animal Studies Tell Us about the Mechanism of Myopia-Protection by
924 Light? *Optom Vis Sci* **93**, 1049-51 (2016).
925 84. Weiss, S. & Schaeffel, F. Diurnal growth rhythms in the chicken eye: relation to myopia
926 development and retinal dopamine levels. *J Comp Physiol A* **172**, 263-70 (1993).
927 85. Stone, R.A., Lin, T., Iuvone, P.M. & Laties, A.M. Postnatal control of ocular growth:
928 dopaminergic mechanisms. *Ciba Found Symp* **155**, 45-57; discussion 57-62 (1990).
929 86. Morgan, I.G. The biological basis of myopic refractive error. *Clin Exp Optom* **86**, 276-88 (2003).
930 87. Li, X.X., Schaeffel, F., Kohler, K. & Zrenner, E. Dose-dependent effects of 6-hydroxy dopamine
931 on deprivation myopia, electroretinograms, and dopaminergic amacrine cells in chickens. *Vis*
932 *Neurosci* **9**, 483-92 (1992).
933 88. Iuvone, P.M., Tigges, M., Stone, R.A., Lambert, S. & Laties, A.M. Effects of apomorphine, a
934 dopamine receptor agonist, on ocular refraction and axial elongation in a primate model of
935 myopia. *Invest Ophthalmol Vis Sci* **32**, 1674-7 (1991).
936 89. Ashby, R., McCarthy, C.S., Maleszka, R., Megaw, P. & Morgan, I.G. A muscarinic cholinergic
937 antagonist and a dopamine agonist rapidly increase ZENK mRNA expression in the form-
938 deprived chicken retina. *Exp Eye Res* **85**, 15-22 (2007).
939 90. Ashby, R. Animal Studies and the Mechanism of Myopia-Protection by Light? *Optom Vis Sci* **93**,
940 1052-4 (2016).
941 91. Rymer, J. & Wildsoet, C.F. The role of the retinal pigment epithelium in eye growth regulation
942 and myopia: a review. *Vis Neurosci* **22**, 251-61 (2005).
943 92. Chen, S. *et al.* Bright Light Suppresses Form-Deprivation Myopia Development With Activation
944 of Dopamine D1 Receptor Signaling in the ON Pathway in Retina. *Invest Ophthalmol Vis Sci* **58**,
945 2306-2316 (2017).
946 93. Chen, P.S. *et al.* Effects of C825T polymorphism of the GNB3 gene on availability of dopamine
947 transporter in healthy volunteers--a SPECT study. *Neuroimage* **56**, 1526-30 (2011).
948 94. Scott, M.S. & Ono, M. From snoRNA to miRNA: Dual function regulatory non-coding RNAs.
949 *Biochimie* **93**, 1987-92 (2011).

950 95. McFadden, S.A. Understanding and Treating Myopia: What More We Need to Know and Future
951 Research Priorities. *Optom Vis Sci* **93**, 1061-3 (2016).
952 96. Smith, E.L., 3rd, Hung, L.F. & Arumugam, B. Visual regulation of refractive development:
953 insights from animal studies. *Eye (Lond)* **28**, 180-8 (2014).
954 97. Zhang, Y. & Wildsoet, C.F. RPE and Choroid Mechanisms Underlying Ocular Growth and
955 Myopia. *Prog Mol Biol Transl Sci* **134**, 221-40 (2015).
956 98. Harper, A.R. & Summers, J.A. The dynamic sclera: extracellular matrix remodeling in normal
957 ocular growth and myopia development. *Exp Eye Res* **133**, 100-11 (2015).
958 99. Summers, J.A. The choroid as a sclera growth regulator. *Exp Eye Res* (2013).
959 100. Howie, B., Fuchsberger, C., Stephens, M., Marchini, J. & Abecasis, G.R. Fast and accurate
960 genotype imputation in genome-wide association studies through pre-phasing. *Nat Genet* **44**, 955-
961 9 (2012).
962 101. Marchini, J., Howie, B., Myers, S., McVean, G. & Donnelly, P. A new multipoint method for
963 genome-wide association studies by imputation of genotypes. *Nat Genet* **39**, 906-13 (2007).
964 102. van Leeuwen, E.M. *et al.* Population-specific genotype imputations using minimac or IMPUTE2.
965 *Nat Protoc* **10**, 1285-96 (2015).
966 103. Aulchenko, Y.S., Struchalin, M.V. & van Duijn, C.M. ProbABEL package for genome-wide
967 association analysis of imputed data. *BMC Bioinformatics* **11**, 134 (2010).
968 104. Chen, W.M. & Abecasis, G.R. Family-based association tests for genomewide association scans.
969 *Am J Hum Genet* **81**, 913-26 (2007).
970 105. Winkler, T.W. *et al.* Quality control and conduct of genome-wide association meta-analyses. *Nat*
971 *Protoc* **9**, 1192-212 (2014).
972 106. Willer, C.J., Li, Y. & Abecasis, G.R. METAL: fast and efficient meta-analysis of genomewide
973 association scans. *Bioinformatics* **26**, 2190-1 (2010).
974 107. Zaykin, D.V. Optimally weighted Z-test is a powerful method for combining probabilities in
975 meta-analysis. *J Evol Biol* **24**, 1836-41 (2011).
976 108. Whitlock, M.C. Combining probability from independent tests: the weighted Z-method is
977 superior to Fisher's approach. *J Evol Biol* **18**, 1368-73 (2005).
978 109. Dudbridge, F. & Gusnanto, A. Estimation of significance thresholds for genomewide association
979 scans. *Genet Epidemiol* **32**, 227-34 (2008).
980 110. Pruim, R.J. *et al.* LocusZoom: regional visualization of genome-wide association scan results.
981 *Bioinformatics* **26**, 2336-7 (2010).
982 111. Yang, H. & Wang, K. Genomic variant annotation and prioritization with ANNOVAR and
983 wANNOVAR. *Nat Protoc* **10**, 1556-66 (2015).
984 112. Cooper, G.M. *et al.* Distribution and intensity of constraint in mammalian genomic sequence.
985 *Genome Res* **15**, 901-13 (2005).
986 113. Schwarz, J.M., Rodelsperger, C., Schuelke, M. & Seelow, D. MutationTaster evaluates disease-
987 causing potential of sequence alterations. *Nat Methods* **7**, 575-6 (2010).
988 114. Loh, P.R. *et al.* Efficient Bayesian mixed-model analysis increases association power in large
989 cohorts. *Nat Genet* **47**, 284-90 (2015).
990 115. McCarthy, S. *et al.* A reference panel of 64,976 haplotypes for genotype imputation. *Nat Genet*
991 **48**, 1279-83 (2016).
992 116. Consortium, G.T. Human genomics. The Genotype-Tissue Expression (GTEx) pilot analysis:
993 multitissue gene regulation in humans. *Science* **348**, 648-60 (2015).
994 117. Chang, C.C. *et al.* Second-generation PLINK: rising to the challenge of larger and richer datasets.
995 *Gigascience* **4**, 7 (2015).
996 118. Amberger, J., Bocchini, C.A., Scott, A.F. & Hamosh, A. McKusick's Online Mendelian
997 Inheritance in Man (OMIM). *Nucleic Acids Res* **37**, D793-6 (2009).
998 119. Bauer-Mehren, A., Rautschka, M., Sanz, F. & Furlong, L.I. DisGeNET: a Cytoscape plugin to
999 visualize, integrate, search and analyze gene-disease networks. *Bioinformatics* **26**, 2924-6 (2010).

1000 120. Gunther, S. *et al.* SuperTarget and Matador: resources for exploring drug-target relationships.
1001 *Nucleic Acids Res* **36**, D919-22 (2008).
1002 121. Kuhn, M. *et al.* STITCH 4: integration of protein-chemical interactions with user data. *Nucleic*
1003 *Acids Res* **42**, D401-7 (2014).
1004 122. Wishart, D.S. *et al.* DrugBank: a comprehensive resource for in silico drug discovery and
1005 exploration. *Nucleic Acids Res* **34**, D668-72 (2006).
1006 123. Whirl-Carrillo, M. *et al.* Pharmacogenomics knowledge for personalized medicine. *Clin*
1007 *Pharmacol Ther* **92**, 414-7 (2012).
1008
1009

1010
1011

1012 **Figure 1. GWAS meta-analysis identifies 140 loci for refractive error (Stage 3)**

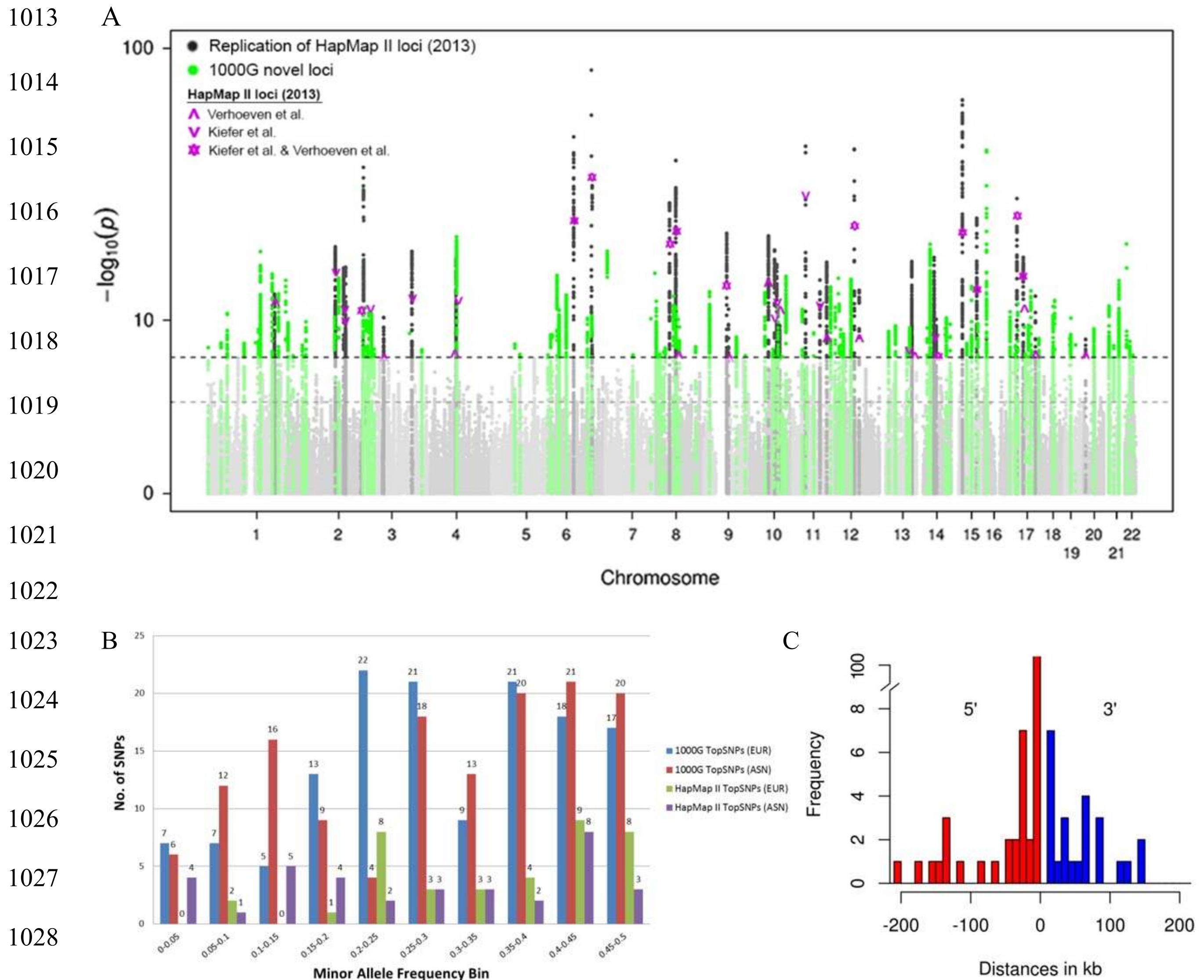

1030 **(a)** We conducted a meta-analysis of genome-wide single-variant analyses for >10 million variants in
1031 160,420 participants of CREAM and 23andMe (Stage 3). Shown is the Manhattan plot depicting *P* values
1032 for association, highlighting new ($P < 5 \times 10^{-8}$ for the first time; green) and known (dark grey) refractive
1033 error loci previously found using HapMap II imputations from Kiefer et al.[27] and Verhoeven et al.[26]
1034 (**Table 1**). The horizontal lines indicate suggestive significance ($P = 1 \times 10^{-5}$) or genome-wide

1035 significance ($P = 5 \times 10^{-8}$). **(b)** We compared the minor allele frequencies of the 140 discovered index
1036 variants based on 1000G (blue: Europeans; red: Asians) to the minor allele frequencies of the previously
1037 found genetic variants based on HapMap II (green: Europeans; purple: Asians). Observed are an increase
1038 in genetic variants found across all minor allele frequency bins increase, including the lower minor allele
1039 frequency bins. **(c)** We annotated the 167 loci to genes using wANNOVAR. Shown are the distances
1040 between index variants from the nearest gene and its gene on the 5' and/or 3' site. The majority of index
1041 variants (84%) were at a distance of less than 50 kb up- or downstream from the annotated gene.

1042
1043

Table 1. Results of the meta-analysis of CREAM and 23andMe for the previously-identified loci and a subset of the newly-identified loci, and replication in UK Biobank

Table 1a Replication of the HapMap II index variants for refractive error per locus in the Stage 3 meta-analysis

SNP	Chr.	Position	Nearest Loci And Gene(s)	Effect Allele	Other Allele	EAF EUR	EAF ASN	Z-score	Direction	P value	HetISq	HetPVal	Sample Size (N)	HapMap II Discovery (2013)	Category (I = both GWS in Stage 1 and 2, 2=one of two cohorts (CREAM or 23andMe) GWS, 3= both not GWS in Stage 1 or 2)	P value Replication UKBB
rs10500355	16	7459347	RBFOX1	A	T	0.354	0.1334	-13.73	--	6.49E-43	9.1	2.93E-07	160139	Kiefer et al. & Verhoeven et al.	I	2.50E-48
rs11145465	9	71766593	TJP2	A	C	0.212	NA	-9.55	--	1.35E-21	46.3	0.1722	153174	Kiefer et al. & Verhoeven et al.	I	1.00E-10
rs11178469	12	71275137	PTPRR	T	C	0.752	0.6384	-7.40	--	1.33E-13	0	0.6989	160139	Verhoeven et al.	II (CREAM)	2.60E-04
rs11602008	11	40149305	LRRC4C	A	T	0.822	0.7488	13.98	++	2.12E-44	22.5	1.56E-10	157505	Kiefer et al.	II (23andMe)	2.90E-47
rs12193446	6	129820038	BC035400, LAMA2	A	G	0.906	NA	-19.43	--	4.21E-84	16.8	5.72E-15	150269	Kiefer et al. & Verhoeven et al.	I	4.60E-106
rs1550094	2	233385396	CHRNG,PRSS56	A	G	0.701	0.705	12.74	++	3.64E-37	26.3	0.002705	159422	Kiefer et al. & Verhoeven et al., Kiefer et al.	I	4.10E-59
rs1649068	10	60304864	BICC1	A	C	0.475	0.5044	-9.44	--	3.77E-21	0	0.7118	160144	Verhoeven et al.	I	7.50E-11
rs17382981	10	94953258	CYP26A1,MYOF	T	C	0.417	0.1901	-6.31	--	2.72E-10	67.9	0.07737	155332	Verhoeven et al.	II (CREAM)	4.10E-07
rs17428076	2	172851936	HAT1,METAP1D	C	G	0.768	0.8542	-8.18	--	2.77E-16	0	0.002854	160151	Kiefer et al.	II (23andMe)	7.50E-08
rs1858001	1	207488004	C4BPA,CD55	C	G	0.676	0.4151	7.28	++	3.45E-13	59.6	0.02007	160149	Verhoeven et al.	II (CREAM)	6.70E-20
rs1954761	11	105596885	GRIA4	T	C	0.371	0.3772	-8.40	--	4.57E-17	0	0.911	160122	Verhoeven et al.	I	1.20E-16
rs2155413	11	84634790	DLG2	A	C	0.482	0.6549	-7.76	--	8.85E-15	0	0.0002987	159504	Kiefer et al.	II (23andMe)	1.10E-17
rs235770	20	6761765	BMP2	T	C	0.372	0.3875	-5.93	--	3.11E-09	0	0.5474	157521	Verhoeven et al.	II (23andMe)	4.80E-11
rs2573081	2	178828507	PDE11A	C	G	0.524	0.5378	8.21	++	2.18E-16	47.6	0.1672	160126	Kiefer et al.	II (23andMe)	1.60E-29
rs2753462	14	60850703	JB175233,C14orf39	C	G	0.296	0.5679	-6.49	--	8.37E-11	73.9	0.05032	157352	Verhoeven et al.	II (CREAM)	2.00E-15
rs2855530	14	54421917	BMP4	C	G	0.507	0.4736	-8.58	--	9.87E-18	41.7	0.1904	160092	Kiefer et al.	I	4.80E-22
rs2908972	17	11407259	SHISA6	A	T	0.415	0.4879	-11.13	--	9.46E-29	23	0.2544	160123	Kiefer et al. & Verhoeven et al.	I	6.10E-29
rs3138141	12	56115778	BLOC1S1-RDH5,RDH5	A	C	0.214	0.1472	13.80	++	2.46E-43	3.2	5.05E-07	157531	Kiefer et al. & Verhoeven et al.	I	2.30E-56
rs4687586	3	53837971	CACNA1D	C	G	0.691	NA	-6.55	--	5.86E-11	0	0.6046	150217	Verhoeven et al.	III	1.60E-08
rs4793501	17	68718734	KCNJ2,BC039327	T	C	0.575	0.444	-7.21	--	5.53E-13	0	0.5917	160150	Verhoeven et al.	II (CREAM)	3.70E-12
rs524952	15	35005886	GOLGA8B,GJD2	A	T	0.475	0.5077	-17.08	--	2.28E-65	67.2	0.01544	160150	Kiefer et al. & Verhoeven et al.	I	1.60E-103
rs56075542	2	146882415	BC040861,PABPC1P2	T	G	0.552	0.4726	-8.99	--	2.39E-19	13.9	0.001284	159478	Kiefer et al.	II (23andMe)	1.30E-18
rs62070229	17	31227593	MYO1D,TMEM98	A	G	0.807	0.8747	8.58	++	9.64E-18	0	0.4158	156570	Verhoeven et al.	I	1.30E-18
rs6495367	15	79375347	RASGRF1	A	G	0.408	0.3988	-10.20	--	1.95E-24	0	0.667	160144	Kiefer et al. & Verhoeven et al.	I	7.20E-37
rs7042950	9	77149837	RORB	A	G	0.732	0.3924	6.80	++	1.07E-11	0	0.9122	160153	Verhoeven et al.	III	2.90E-18
rs72621438	8	60178580	SNORA51,CA8	C	G	0.642	0.6089	-13.14	--	2.03E-39	38.4	0.00559	160128	Kiefer et al. & Verhoeven et al.	I	1.80E-49
rs745480	10	85986554	LRIT2,LRIT1	C	G	0.511	0.4182	8.31	++	9.26E-17	67.3	0.0805	159504	Kiefer et al.	II (23andMe)	8.20E-18
rs7624084	3	141093285	ZBTB38	T	C	0.568	0.6332	-8.81	--	1.24E-18	18.5	0.01802	160151	Kiefer et al.	II (23andMe)	6.50E-17
rs7662551	4	80537638	LOC100506035,PCAT4	A	G	0.723	0.5577	8.53	++	1.47E-17	19.4	0.2653	160147	Verhoeven et al.	I	6.00E-12
rs7692381	4	81903049	C4orf22,BMP3	A	G	0.763	0.6308	9.40	++	5.55E-21	0	0.01253	160134	Kiefer et al.	I	7.50E-13
rs7744813	6	73643289	KCNQ5	A	C	0.591	0.6017	-14.56	--	5.43E-48	35	0.001132	160091	Kiefer et al. & Verhoeven et al.	I	1.00E-75
rs7829127	8	40726394	ZMAT4	A	G	0.792	0.8974	-10.91	--	1.02E-27	15.9	0.0002774	160132	Kiefer et al. & Verhoeven et al.	II (23andMe)	3.10E-22
rs7895108	10	79061458	KCNMA1	T	G	0.351	0.1182	-8.87	--	7.56E-19	32.8	0.02115	160140	Kiefer et al.	II (23andMe)	1.10E-27
rs79266634	16	7309047	RBFOX1	C	G	0.093	0.1151	-5.93	--	3.00E-09	0	0.5614	156268	Kiefer et al. & Verhoeven et al.	III	1.50E-08
rs837323	13	101175664	PCCA	T	C	0.512	0.7625	6.32	++	2.65E-10	35.6	0.2129	160142	Verhoeven et al.	II (23andMe)	5.30E-16
rs9517964	13	100717833	ZIC2,PCCA	T	C	0.589	0.786	8.42	++	3.68E-17	0	0.01962	160121	Kiefer et al.	II (23andMe)	3.40E-20

Table 1b Subset of the new loci harboring the smallest p-values for refractive error in the Stage 3 meta-analysis

SNP	Chr.	Position	Nearest Loci And Gene(s)	Effect Allele	Other Allele	EAF EUR	EAF ASN	Z-score	Direction	P value	HetISq	HetPVal	Sample Size (N)	Category (I = both GWS in Stage 1 and 2, 2=one of two cohorts (CREAM or 23andMe) GWS, 3= not GWS in Stage 1 or 2)	P value Replication UKBB
rs36024104	14	42294993	LRFN5	A	G	0.823	NA	9.09	++	9.86E-20	15.9	0.01414	152585	II (23andMe)	2.20E-12
rs7456039	7	6901710	CCZ1B,LOC100131257	C	G	0.183	NA	8.82	++	1.18E-18	42.1	3.79E-12	121337	II (23andMe)	6.50E-01
rs1556867	1	164213686	5S_rRNA,PBX1	T	C	0.264	0.494	-8.81	--	1.29E-18	71.1	0.06266	160155	II (23andMe)	4.20E-17
rs12667032	7	154406581	DPP6	A	G	0.152	0.317	7.99	++	1.31E-15	82.3	1.02E-11	130790	II (23andMe)	2.10E-01
rs2225986	1	200311910	LINC00862	A	T	0.381	0.169	-7.96	--	1.68E-15	40.2	0.196	160152	II (23andMe)	7.50E-17
rs1207782	6	22059967	LINC00340	T	C	0.577	0.265	-7.92	--	2.47E-15	0	0.8946	160149	I	4.90E-13
rs72826094	10	114801488	TCF7L2	A	T	0.799	0.838	7.88	++	3.20E-15	64.5	0.09323	156825	II (23andMe)	4.90E-02
rs297593	2	157363743	GPD2	T	C	0.286	0.257	-7.82	--	5.45E-15	0	0.5285	159461	II (23andMe)	7.80E-11
rs5442	12	6954864	GNB3	A	G	0.068	NA	-7.82	--	5.48E-15	8.8	0.03693	146217	II (23andMe)	1.20E-33
rs10880855	12	46144855	ARID2	T	C	0.507	0.464	-7.78	--	7.35E-15	0	0.9683	160144	I	4.80E-08
rs12405776	1	242431557	PLD5	T	C	0.220	0.521	7.75	++	9.52E-15	64.9	3.56E-10	153784	II (23andMe)	1.50E-01
rs2150458	21	47377296	PCBP3,COL6A1	A	G	0.455	0.641	7.74	++	1.04E-14	55.7	0.1329	160151	II (23andMe)	1.80E-13
rs12898755	15	63574641	APH1B	A	G	0.245	0.456	7.53	++	4.98E-14	7.9	0.2974	159506	II (23andMe)	1.40E-16
rs7122817	11	117657679	DSCAML1	A	G	0.507	0.662	7.51	++	5.73E-14	73.8	0.05077	160147	II (23andMe)	1.10E-10
rs10511652	9	18362865	SH3GL2,ADAMTSL1	A	G	0.416	0.445	7.36	++	1.91E-13	44.8	0.1782	160149	II (23andMe)	3.50E-18
rs11101263	10	49414181	FRMPD2	T	C	0.258	0.105	-7.33	--	2.33E-13	0	0.3477	160155	II (23andMe)	2.20E-13
rs11118367	1	219790221	LYPLAL1	T	C	0.482	0.630	-7.29	--	3.16E-13	0	0.8576	160141	III	1.20E-13
rs9395623	6	50757699	TFAP2D,TFAP2B	A	T	0.315	0.381	7.25	++	4.16E-13	0	0.9579	160151	III	2.20E-10
rs284816	8	53362145	ST18,FAM150A	A	G	0.163	0.198	-7.21	--	5.52E-13	0	0.9242	160140	III	1.60E-08
rs12965607	18	47391025	MYO5B	T	G	0.857	0.923	7.07	++	1.52E-12	20.8	0.01674	157604	II (23andMe)	8.10E-16
rs7747	4	80827062	ANTXR2	T	C	0.202	0.093	7.03	++	2.05E-12	5.4	0.01267	150327	II (23andMe)	7.70E-16
rs12451582	17	54734643	NOG,C17orf67	A	G	0.369	0.308	7.02	++	2.22E-12	0	0.5925	160155	II (23andMe)	8.80E-18
rs80253120	17	14138507	CDRT15	T	C	0.626	0.723	6.97	++	3.25E-12	58.6	0.12	156054	II (23andMe)	7.20E-11
22:23069851:I	22	23069851	DKFZp667J0810,abParts	ATG	A	0.084	0.1582	6.95	-+	3.56E-12	98.5	4.80E-16	120481	II (23andMe)	9.30E-01
rs7968679	12	9313304	PZP	A	G	0.700	0.894	6.95	++	3.65E-12	0	0.01951	160076	II (23andMe)	4.20E-10
rs11202736	10	90142203	RNLS	A	T	0.717	0.762	-6.92	--	4.53E-12	0	0.4007	160150	II (23andMe)	9.40E-07
rs11088317	21	16574122	NRIP1,USP25	T	C	0.287	0.299	-6.90	--	5.38E-12	72.5	0.05657	160116	II (23andMe)	6.50E-06
rs10853531	18	42824449	SLC14A2	A	G	0.200	0.182	6.88	++	5.89E-12	0	0.6755	160104	III	2.60E-10
rs72655575	8	60556509	SNORA51,CA8	A	C	0.201	0.124	6.87	++	6.54E-12	0	0.8811	156566	I	7.10E-07
rs12998513	2	242879499	CXXC11,AK097934	A	G	0.880	0.676	-6.86	+-	7.15E-12	65.2	4.51E-14	117611	II (23andMe)	7.80E-01
rs1790165	11	131928971	NTM	A	C	0.411	0.283	6.85	++	7.17E-12	0	0.003708	160131	II (23andMe)	1.80E-10
rs511217	11	30029948	METTL15,KCNA4	A	T	0.738	0.729	-6.79	--	1.10E-11	0	0.3626	160143	II (23andMe)	1.40E-17
rs1150687	6	28162469	ZNF192P1,TRNA_Ser	T	C	0.619	0.504	6.78	++	1.17E-11	56.2	0.131	159448	II (23andMe)	3.10E-10
rs56055503	16	80532694	MAF,DYNLRB2	A	G	0.751	0.539	-6.72	--	1.83E-11	0	0.8407	160145	II (23andMe)	8.00E-06
rs9681162	3	8194734	AK124857,LMCD1-AS1	T	C	0.680	0.437	6.70	++	2.10E-11	63	0.1002	160152	II (23andMe)	6.30E-13
rs11589487	1	61342229	AK097193,BC030753	A	G	0.445	0.089	6.67	++	2.64E-11	34.6	0.2163	160143	II (23andMe)	2.20E-10

We identified 140 loci for refractive error with genome-wide significance (P < 5 × 10−8) on the basis the meta-analyses of the genome-wide single-variant linear regressions performed in 160,420 participants of mixed ancestries (CREAM-ASN, CREAM-EUR and 23andMe). Shown are the replication of the previously found loci from HapMap II and a subset of the new loci harboring the smallest p-values. For each locus, represented by an index variant (the variant with smallest p-value in that locus), Effect Allele, Other Allele, effect allele frequencies per ancestry (EAF AZN and EAF EUR), effect size (Z-score), direction of the effect (Direction), the P value, heterogeneity I square (HetISq), heterogeneity P value (HetPval), Sample Size (N), Category and P value of the replication in UK Biobank are shown (Full table: Supplementary Excel Table 1). Chr., chromosome; EAF, effect allele frequency; ASN, Asian; EUR, European; GWS, genome wide significant; UKBB, United Kingdom Biobank.

1049
1050
1051
1052

1053

1054 **Figure 2. Correlation of statistical significance and effect size of SNPs based on spherical equivalent**

1055 **(SphE) in diopters and age of diagnosis of myopia (AODM) in years.**

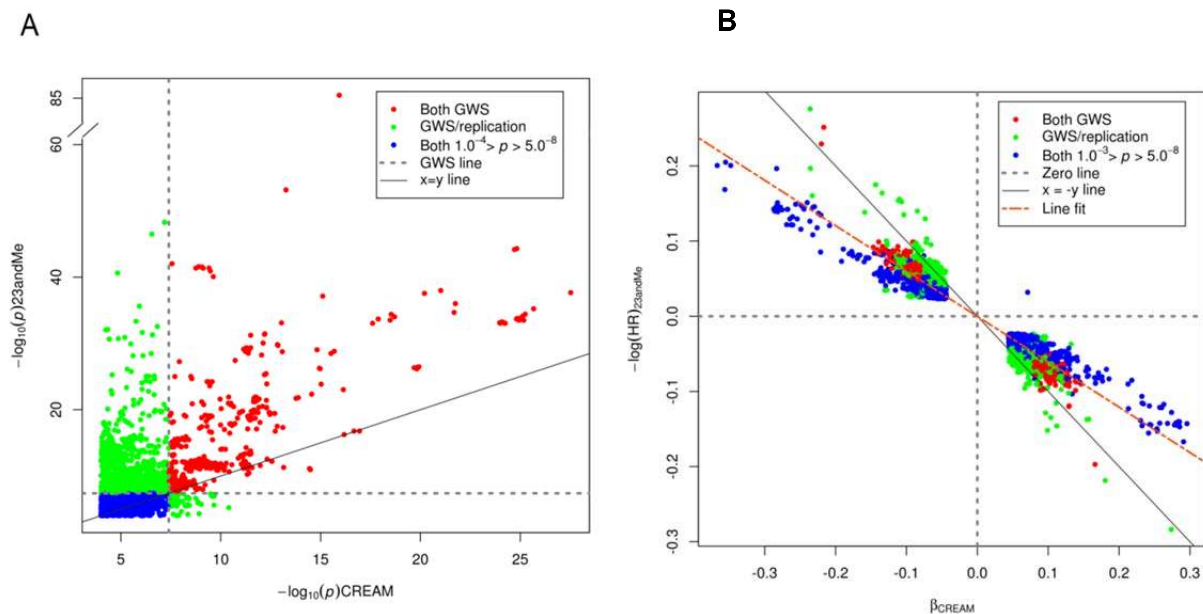

1056

1057

1058 **(a)** *P* value per genetic variant comparison between CREAM meta-analysis (Stage 1) and 23andMe

1059 (Stage 2) meta-analysis. Shown is the overlap (red) and the difference (green) in *P* value signals per

1060 cohort for genetic variants. Green genetic variants are only genome wide significant in either CREAM or

1061 23andMe. Blue: genetic variants with P value between 5.0 x 10^{-8} and 1.0 x 10^{-3} in both CREAM and

1062 23andMe. **(b)** Comparison of effects (SphE and logHR of AODM in years) between CREAM and

1063 23andMe. Same color code was applied as in (a). The effects were concordant in their direction of effect

1064 on refractive error. The regression slope is -0.15 diopters per logHR of AODM in years.

1065 **Figure 3. Risk of refractive error per decile of polygenic risk score (Rotterdam Study I-III, N =**

1066 **10,792)**

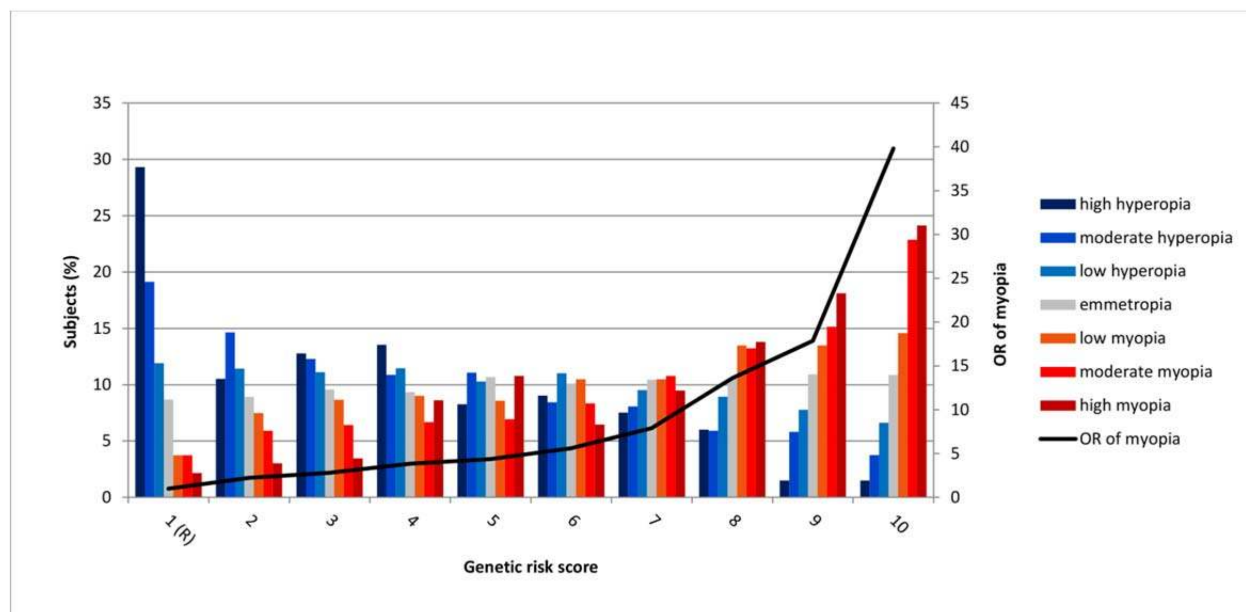

1067

1068 Distribution of refractive error in subjects from Rotterdam Study I–III (*N* = 10,792) as a function

1069 of the optimal polygenic risk score (including 7,303 variants at *P* value ≤ 0.005 explaining 7.8% of the

1070 variance of SphE; Supplementary Table 9). Mean OR of myopia (black line) was calculated per polygenic

1071 risk score category using the lowest category as a reference. High myopia (SphE ≤-6 D), moderate

1072 myopia (SphE >-6 D & ≤ −3 D), low myopia (SphE > −3 D & <-1.5 D), emmetropia (SphE ≥ −1.5 D and

1073 ≤ 1.5 D), low hyperopia (SphE > 1.5 D & < 3 D), moderate hyperopia (SphE ≥ 3 D & 6 D), high

1074 hyperopia (SphE ≥ 6 D).

1075

1076 **Table 1. Genetic correlation for refractive error between Europeans and East Asians**

Sample 1	**Sample 2**	**Genetic effect correlation (*pge*) [a]**	**Genetic impact correlation (*pgi*) [a]**
EUR CREAM	**EAS CREAM**	**0.804 (se=0.041) P = 1.83 x 10^{-6}**	**0.888 (se=0.061) P = 0.065**
EUR 23andMe	**EAS CREAM**	**0.788 (se=0.041) P = 2.48 x 10^{-7}**	**0.865 (se=0.054) P = 0.014**
Abbreviations: EUR, European; EAS, East Asian.			
[a] P-value relates to a test of the null hypothesis that *pge*=1 or *pgi*=1.			

1077

1078 We calculated the genetic correlation of effect (pge) and impact (pgi) using Popcorn to compare the

1079 genetic associations between Europeans (CREAM-EUR, N= 44,192; 23andMe, N=104,292) and East

1080 Asians (CREAM-ASN, N= 9,826). Reference panels for Popcorn were constructed using genotype data

1081 for 503 EUR and 504 EAS individuals sequenced as part of the 1000 Genomes Project. SNPs used had a

1082 MAF of at least 5% in both populations, resulting in a final set of 3,625,602SNPs for the analyses using

1083 the 23andMe GWAS sample and 3,642,928 SNPs for those using the CREAM-EUR sample. These

1084 findings support a largely common genetic predisposition to refractive error and myopia in Europeans and

1085 Asians, although ancestry-specific risk alleles may exist.

1086 **Figure 4. Visualization of the DEPICT gene-set enrichment analysis based on loci associated with**

1087 **refractive error and the correlation between the (meta)gene sets**

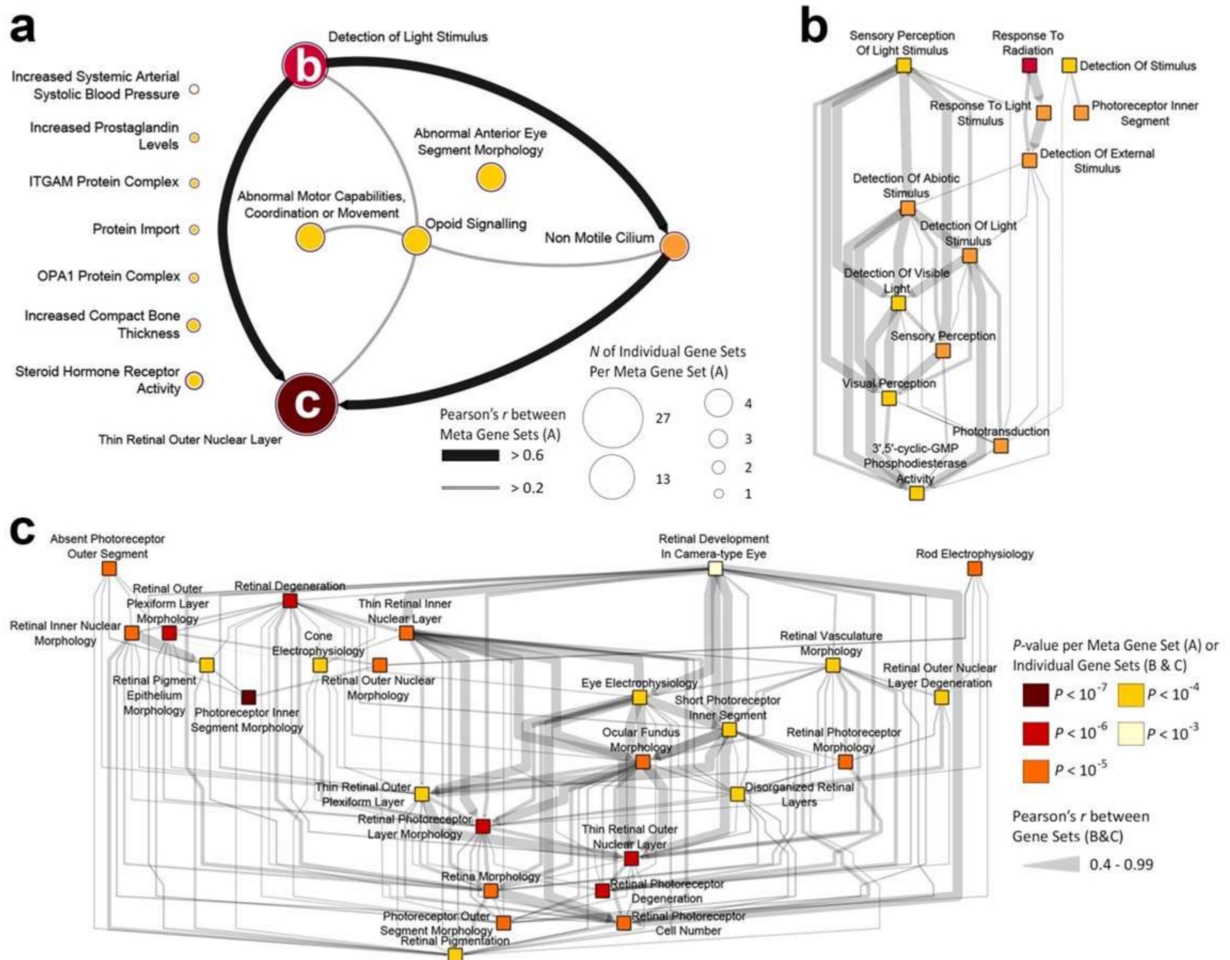

1088

1089 **(a)** Shown are the 66 gene sets clustered into thirteen meta gene sets based on the gene set enrichment

1090 analysis of DEPICT (*P* value < 1 × 10−5 in the GWAS, FDR < 0.05). **(b)** Visualization of the

1091 interconnectivity between gene sets (n=13) of the meta gene set 'Detection of Light Stimulus'

1092 (GO:0009583). **(c)** Visualization of the interconnectivity between gene sets (n=27) of the largest meta

1093 gene set 'Thin Retinal Outer Nuclear Layer' (MP:0008515). In all panels, (meta)gene sets are represented

1094 by nodes colored according to statistical significance, and similarities between them are indicated by

1095 edges scaled according to their correlation; r ≥ 0.2 are shown in panel **(a)** and r ≥ 0.4 are shown in panel

1096 **(b,c).**

Table 2. Genes ranked according to biological and statistical evidence

			ANNOTATION*				EXPRESSION			BIOLOGY		PATHWAYS			
Score	Σ	1	1	1	1	1	1	1	1	1	1	1	1	1	
Locus	Gene Priority Score	Internal Replication (≥2 cohorts)	Exonic: Protein Altering	Exonic: Non-Protein Altering	5'or 3' UTR	RNA (nc, sno, linc, other)	eQTL	Expression in human adult ocular tissue	Expression in human developing ocular tissue (fetal - 24 weeks)	Ocular phenotype in mice	Ocular phenotype in human	DEPICT gene-set enrichment	DEPICT gene prioritization	IPA Canonical Pathways	Known Drug Target
GNB3	8														
RDH5	7														
CYP26A1	7														
EFEMP1	7														
GRIA4	7														
RGR	7														
RORB	7														
RCBTB1	6														
MAF	6														
ZEB2	6														
KCNMA1	6														
TJP2	6														
ST18	6														
FBN1	6														
KCNJ2	6														
GJD2	6														
CABP4	6														
TCF7L2	6														
PRSS56	6														

Genes were ranked (orange) based on 10 equal categories which can be divided in four categories: internal replication of genetic variant in more than two cohorts (purple; CREAM-EUR, CREAM-ASN and/or 23andMe), annotation (light blue; genetic variant harboring an exonic protein altering variant or non-protein altering variant, genetic variant residing in a 5' or 3' UTR region of a gene or transcribing an RNA structure), expression (yellow; eQTL, expression in adult human ocular tissue, expression in developing ocular tissue), biology (dark yellow; ocular phenotype in mice, ocular phenotype in humans), pathways (green; DEPICT gene-set enrichment, DEPICT gene prioritization analysis and canonical pathway analysis of IPA). We assessed genes harboring drug targets (salmon red), but did not assign a scoring point to this category.

*Only one point can be assigned in the category 'ANNOTATION', even though it has four columns (i.e. a genetic variant is located in only 1 of these four categories).

1111 **Figure 5. Top molecular network identified by Ingenuity Pathway Analysis (IPA)**

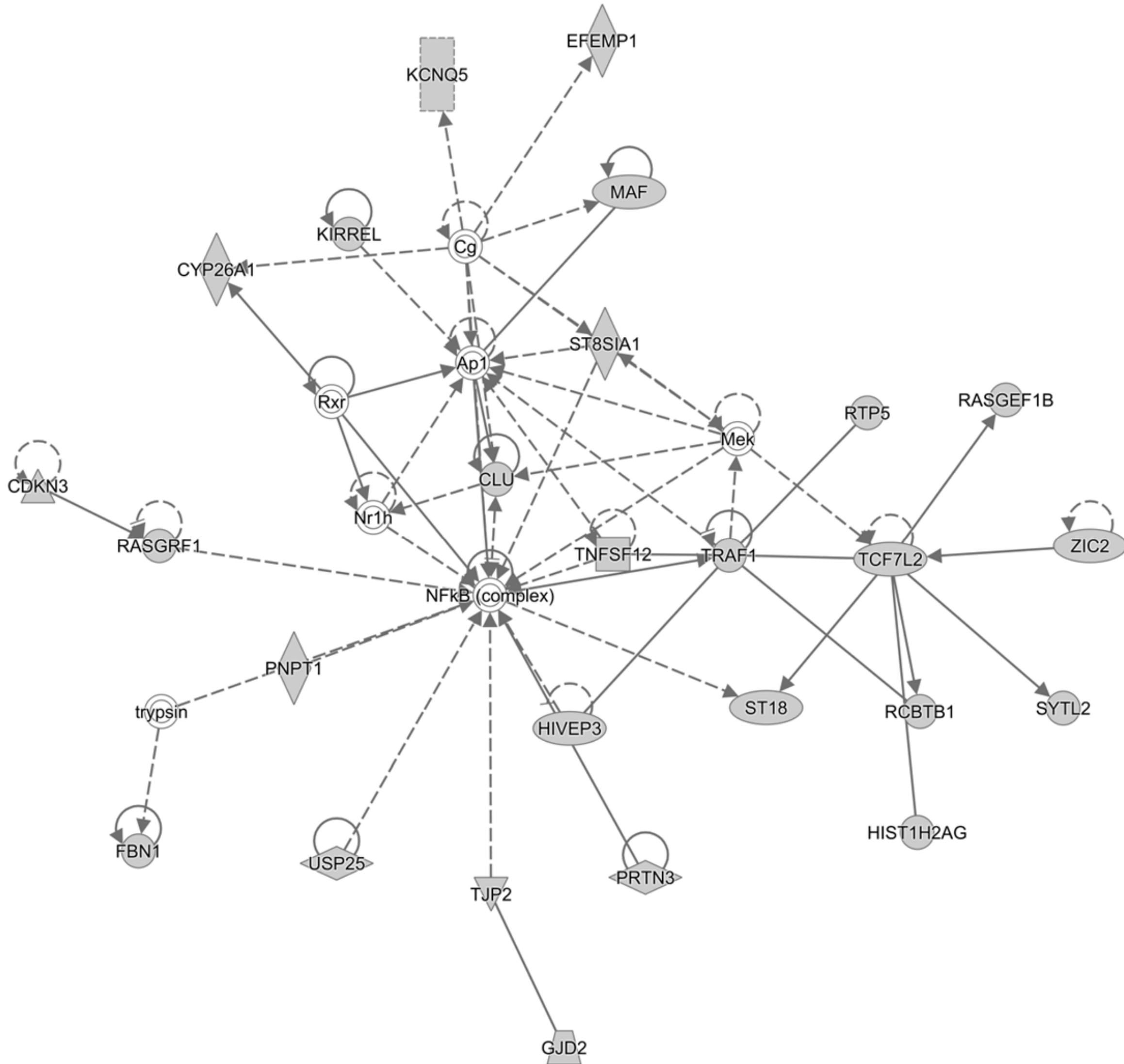

1112

1113

1114 The genes annotated to the top hits identified at Stage 3 were mapped to networks and pathways present

1115 in the IPA database. The most significant network identified by Fisher's exact test was 'Glutamate

1116 Receptor Signaling' (*P* value= 1.56 x 10^{-4}). Genes within the network indicated in grey are genes

1117 associated with refractive error. Other significant pathways are depicted in Supplementary Figure 10.

1118 **Figure 6. Schematic representation of the human eye, retinal cell types, and functional sites of associated genes**

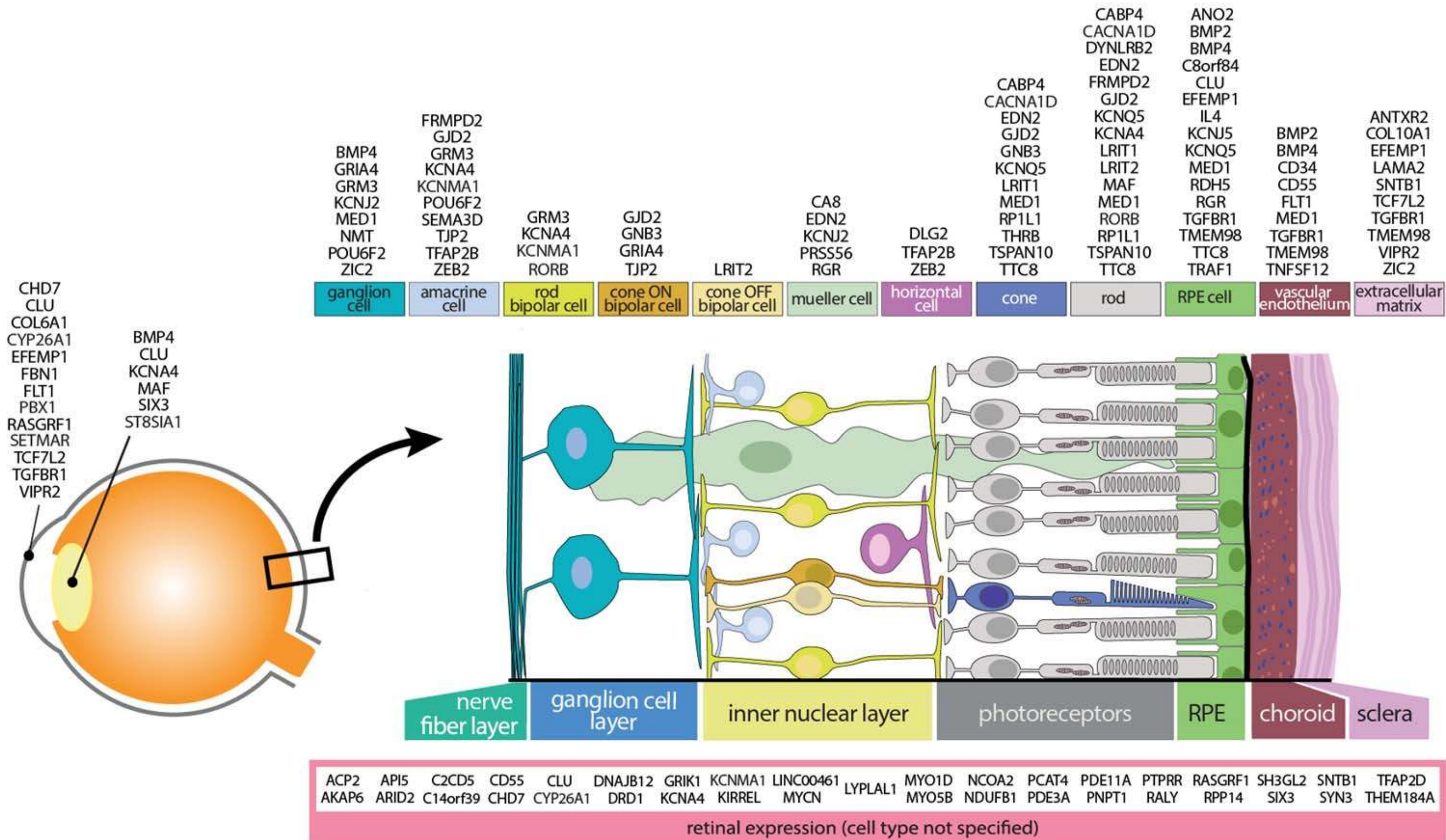

1119

1120 We assessed gene expression sites and/or functional target cells in the eye for all genes using our expression data and literature and data present in

1121 the public domain. The genes appear to be distributed across virtually all cell types in the neurosensory retina, in the RPE, vascular endothelium

1122 and extracellular matrix; i.e., the route of the myopic retina-to-sclera signalling cascade.

1123 **The CREAM Consortium**

1124

1125 Tin Aung[1,2], Joan E. Bailey-Wilson[3], Paul Nigel Baird[4], Amutha Barathi Veluchamy[1,5], Ginevra Biino[6],
1126 Kathryn P. Burdon[7], Harry Campbell[8], Li Jia Chen[9], Peng Chen[2], Wei Chen[10], Ching-Yu Cheng[1,2,5], Emily
1127 Chew[11], Jamie E. Craig[7], Phillippa Cumberland[12,13], Margaret M. Deangelis[14], Cécile Delcourt[15,16],
1128 Xiaohu Ding[17], Angela Döring[18], Cornelia M. van Duijn[19], David M. Evans[20,21], Qiao Fan[22], Lindsay
1129 Farrer[14], Sheng Feng[23], Brian Fleck[24], Rhys D. Fogarty[7], Jeremy R. Fondran[25], Maurizio Fossarello[26], Paul
1130 J. Foster[27,28], Puya Gharahkhani[29], Christian Gieger[18], Adriana I. Iglesias Gonzalez[19,30],, Jeremy A.
1131 Guggenheim[31], Xiaobo Guo[17,32], Toomas Haller[33], Christopher J. Hammond[34,35], Caroline Hayward[36],
1132 Mingguang He[4,17], Alex W. Hewitt[4,37], René Höhn[38], S. Mohsen Hosseini[39], Laura D. Howe[20,40], Pirro G
1133 Hysi[35], Robert P. Igo Jr[25], Sudha K. Iyengar[11,25,41], Sarayut Janmahasatian[25], Vishal Jhanji[9], Jost B.
1134 Jonas[42-44], Mika Kähönen[45], Jaakko Kaprio[46], John P. Kemp[20], Kay-Tee Khaw[47], Anthony P. Khawaja[47],
1135 Chiea-Chuen Khor[2,48-50], Caroline C. W. Klaver[19,30], Barbara E. Klein[51], Ronald Klein[51], Eva Krapohl[52],
1136 Jean-François Korobelnik[15,16], Jonathan H. Lass[25,41], Elisabeth M. van Leeuwen[19,30], Terho Lehtimäki[53],
1137 Yi Lu[29], Robert N. Luben[47], Stuart MacGregor[29], David A. Mackey[4,37], Kari-Matti Mäkelä[53], Nicholas G.
1138 Martin[54], George McMahon[20], Akira Meguro[55], Thomas Meitinger[56], Andres Metspalu[33], Evelin
1139 Mihailov[33], Paul Mitchell[57], Masahiro Miyake[58], Nobuhisa Mizuki[55], Margaux Morrison[14], Vinay
1140 Nangia[59],Songhomitra Panda-Jonas[59], Chi Pui Pang[9], Olavi Pärssinen[60,61], Andrew D. Paterson[39], Norbert
1141 Pfeiffer[38], Mario Pirastu[62], Robert Plomin[52], Ozren Polasek[8,63], Jugnoo S. Rahi[12,13,64], Olli Raitakari[65,66],
1142 Taina Rantanen[60,67], Janina S. Ried[18], Igor Rudan[8], Seang-Mei Saw[1,48], Maria Schache[4], Ilkka Seppälä[53],
1143 George Davey Smith[20], Dwight Stambolian[68], Beate St Pourcain[20,69], Claire L. Simpson[3,70], E-Shyong
1144 Tai[5,48,71], Pancy O. Tam[9], Milly S. Tedja[19,30], Yik-Ying Teo[48,72], J. Willem L. Tideman[19,30], Nicholas J.
1145 Timpson[20], Simona Vaccargiu[62], Zoran Vatavuk[73], Virginie J.M. Verhoeven[19,30], Veronique Vitart[36], Jie
1146 Jin Wang[4,57], Nick J. Wareham[74], Juho Wedenoja[46,75], Cathy Williams[40], Katie M Williams[34,35], James F.
1147 Wilson[8], Robert Wojciechowski[3,76,77], Ya Xing Wang[42,43], Tien-Yin Wong[1,2], Alan F. Wright[36], Jing Xie[4],

1148 Liang Xu[42], Kenji Yamashiro[58], Maurice K.H. Yap[78], Seyhan Yazar[37], Shea Ping Yip[79], Nagahisa

1149 Yoshimura[58], Alvin L. Young[9], Terri L. Young[5,51], Jing Hua Zhao[74], Wanting Zhao[1], Xiangtian Zhou[10]

1150

1151

1152 1. Singapore Eye Research Institute, Singapore National Eye Centre, Singapore, Singapore.
1153 2. Department of Ophthalmology, National University Health Systems, National University of
1154 Singapore, Singapore.
1155 3. Computational and Statistical Genomics Branch, National Human Genome Research Institute,
1156 National Institutes of Health, Baltimore, MD, USA.
1157 4. Centre for Eye Research Australia (CERA), Ophthalmology, Department of Surgery, University
1158 of Melbourne, Royal Victorian Eye and Ear Hospital, Melbourne, Victoria, Australia.
1159 5. Duke-NUS Medical School, Singapore, Singapore.
1160 6. Institute of Molecular Genetics, National Research Council, Pavia, Italy.
1161 7. Department of Ophthalmology, Flinders University, Adelaide, Australia.
1162 8. Centre for Global Health Research, The Usher Institute for Population Health Sciences and
1163 Informatics, University of Edinburgh, Scotland, UK.
1164 9. Department of Ophthalmology and Visual Sciences, The Chinese University of Hong Kong Hong
1165 Kong Eye Hospital, Kowloon, Hong Kong.
1166 10. Department of Radiology, Southwest Hospital, The Third Military Medical University,
1167 Chongqing, China.
1168 11. Department of Genetics, Case Western Reserve University, Cleveland, Ohio, USA.
1169 12. Institute of Child Health, University College London, London, UK.
1170 13. Ulverscroft Vision Research Group, University College London, London, UK.
1171 14. Department of Ophthalmology and Visual Sciences, John Moran Eye Center, University of Utah,
1172 Salt Lake City, Utah, USA.
1173 15. Université de Bordeaux, Bordeaux, France.
1174 16. INSERM (Institut National de la Santé Et de la Recherche Médicale), ISPED (Institut de Santé
1175 Publique d'Épidémiologie et de Développement), Centre INSERM U897-Epidemiologie-
1176 Biostatistique, Bordeaux, France.
1177 17. State Key Laboratory of Ophthalmology, Zhongshan Ophthalmic Center, Sun Yat-sen University,
1178 Guangzhou, China.
1179 18. Institute of Genetic Epidemiology, Helmholtz Zentrum München—German Research Center for
1180 Environmental Health, Neuherberg, Germany.
1181 19. Department of Epidemiology, Erasmus Medical Center, Rotterdam, The Netherlands.
1182 20. MRC Integrative Epidemiology Unit (IEU) at the University of Bristol, Bristol, UK.
1183 21. University of Queensland Diamantina Institute, Translational Research Institute, Brisbane,
1184 Queensland, Australia.
1185 22. Centre for Quantitative Medicine, Duke-NUS Medical School, Singapore, Singapore.
1186 23. Department of Pediatric Ophthalmology, Duke Eye Center For Human Genetics, Durham, North
1187 Carolina, USA.
1188 24. Princess Alexandra Eye Pavilion, Edinburgh, UK.
1189 25. Department of Epidemiology and Biostatistics, Case Western Reserve University, Cleveland,
1190 Ohio, USA.
1191 26. University Hospital 'San Giovanni di Dio', Cagliari, Italy.
1192 27. Division of Genetics and Epidemiology, UCL Institute of Ophthalmology, London, UK.
1193 28. NIHR Biomedical Research Centre, Moorfields Eye Hospital NHS Foundation Trust and UCL
1194 Institute of Ophthalmology, London, UK.
1195 29. Statistical Genetics Laboratory, QIMR Berghofer Medical Research Institute, Herston, Brisbane,
1196 Queensland, Australia.

1197 30. Department of Ophthalmology, Erasmus Medical Center, Rotterdam, The Netherlands.
1198 31. School of Optometry & Vision Sciences, Cardiff University, Cardiff, UK.
1199 32. Department of Statistical Science, School of Mathematics & Computational Science, Sun Yat-
1200 Sen University, Guangzhou.
1201 33. Estonian Genome Center, University of Tartu, Tartu, Estonia.
1202 34. Department of Ophthalmology, King's College London, St Thomas' Hospital campus, London,
1203 UK.
1204 35. Department of Twin Research and Genetic Epidemiology, King's College London School of
1205 Medicine, London, UK.
1206 36. Medical Research Council Human Genetics Unit, Institute of Genetics and Molecular Medicine,
1207 University of Edinburgh, Edinburgh, UK.
1208 37. Centre for Ophthalmology and Visual Science, Lions Eye Institute, University of Western
1209 Australia, Perth, Australia.
1210 38. Department of Ophthalmology, University Medical Center Mainz, Mainz, Germany.
1211 39. Genetics and Genome Biology Program, Hospital for Sick Children and University of Toronto,
1212 Toronto, Ontario, Canada.
1213 40. School of Social and Community Medicine, University of Bristol, Bristol, UK.
1214 41. Department of Ophthalmology and Visual Sciences, Case Western Reserve University and
1215 University Hospitals Eye Institute, Cleveland, Ohio, USA.
1216 42. Beijing Institute of Ophthalmology, Beijing Tongren Hospital, Capital Medical University,
1217 Beijing, China.
1218 43. Beijing Ophthalmology and Visual Science Key Lab, Beijing, China.
1219 44. Department of Ophthalmology, Medical Faculty Mannheim, Ruprecht-Karls-University
1220 Heidelberg, Mannheim, Germany.
1221 45. Department of Clinical Physiology, Tampere University Hospital and School of Medicine,
1222 University of Tampere, Tampere, Finland.
1223 46. Department of Public Health, University of Helsinki, Helsinki, Finland.
1224 47. Department of Public Health and Primary Care, Institute of Public Health, University of
1225 Cambridge School of Clinical Medicine, Cambridge, UK.
1226 48. Saw Swee Hock School of Public Health, National University Health Systems, National
1227 University of Singapore, Singapore, Singapore.
1228 49. Division of Human Genetics, Genome Institute of Singapore, Singapore, Singapore.
1229 50. Department of Ophthalmology and Visual Sciences, University of Utah, Moran Eye Center, Salt
1230 Lake City, USA.
1231 51. Ophthalmology and Visual Sciences, University of Wisconsin-Madison, Madison, WI, USA.
1232 52. MRC Social, Genetic and Developmental Psychiatry Centre, Institute of Psychiatry, Psychology
1233 & Neuroscience, King's College London, London, UK.
1234 53. Department of Clinical Chemistry, Fimlab laboratories and School of Medicine, University of
1235 Tampere, Tampere, Finland.
1236 54. Genetic Epidemiology Laboratory, QIMR Berghofer Medical Research Institute, Herston,
1237 Brisbane, Queensland, Australia.
1238 55. Department of Ophthalmology, Yokohama City University School of Medicine, Yokohama,
1239 Kanagawa, Japan.
1240 56. Institute of Human Genetics, Technical University Munich, Munich, Germany.
1241 57. Centre for Vision Research, Department of Ophthalmology and Westmead Institute for Medical
1242 Research, University of Sydney, Sydney, Australia.
1243 58. Department of Ophthalmology and Visual Sciences, Kyoto University Graduate School of
1244 Medicine, Kyoto, Japan.
1245 59. Suraj Eye Institute, Nagpur, Maharashtra, India.
1246 60. Department of Health Sciences and Gerontology Research Center, University of Jyväskylä,
1247 Jyväskylä, Finland.

1248 61. Department of Ophthalmology, Central Hospital of Central Finland, Jyväskylä, Finland.
1249 62. Institute of Genetic and Biomedic Research, National Research Council, Cagliari, Italy.
1250 63. Faculty of Medicine, University of Split, Split, Croatia.
1251 64. Institute of Ophthalmology, Moorfields Eye Hospital, London, UK.
1252 65. Research Centre of Applied and Preventive Medicine, University of Turku, Turku, Finland.
1253 66. Department of Clinical Physiology and Nuclear Medicine, Turku University Hospital, Turku,
1254 Finland.
1255 67. Gerontology Research Center, University of Jyväskylä, Jyväskylä, Finland.
1256 68. Department of Ophthalmology, University of Pennsylvania, Philadelphia, Pennsylvania, USA.
1257 69. Max Planck Institute for Psycholinguistics, Wundtlaan 1, 6525 XD Nijmegen, The Netherlands.
1258 70. Deptartment of Genetics, Genomics and Informatics, University of Tennessee Health Science
1259 Center, Memphis, TN, USA.
1260 71. Department of Medicine, National University of Singapore, Singapore, Singapore.
1261 72. Department of Statistics and Applied Probability, National University of Singapore, Singapore,
1262 Singapore.
1263 73. Department of Ophthalmology, Sisters of Mercy University Hospital, Zagreb, Croatia.
1264 74. MRC Epidemiology Unit, Institute of Metabolic Sciences, University of Cambridge, Cambridge,
1265 UK.
1266 75. Department of Ophthalmology, Helsinki University Central Hospital, Helsinki, Finland.
1267 76. Department of Epidemiology, Johns Hopkins Bloomberg School of Public Health, Baltimore,
1268 Maryland, USA.
1269 77. Wilmer Eye Institute, Johns Hopkins School of Medicine, Baltimore, MD, USA.
1270 78. Centre for Myopia Research, School of Optometry, The Hong Kong Polytechnic University,
1271 Hong Kong, Hong Kong.
1272 79. Department of Health Technology and Informatics, The Hong Kong Polytechnic University,
1273 Hong Kong, Hong Kong.
1274